ISSN 2355-3286

ULTIMA Computing

Jurnal Sistem Komputer

Engineering | Vol. 15 | No. 1 | Page 1 - 34 | June 2023 | ISSN 2355-3286

UMN

UNIVERSITAS
MULTIMEDIA
NUSANTARA

ISSN 2355-3286

EDITORIAL BOARD

EDITORIAL ADDRESS

Universitas Multimedia Nusantara (UMN)
Jl. Scientia Boulevard
Gading Serpong
Tangerang, Banten - 15811
Indonesia
Phone. (021) 5422 0808
Fax. (021) 5422 0800
Email : ultimacomputing@umn.ac.id

Ultima Computing : Jurnal Sistem Komputer is a Journal of Computer Engineering Study Program, Universitas Multimedia Nusantara which presents scientific research articles in the field of Computer Engineering and Electrical Engineering as well as current theoretical and practical issues, including Edge Computing, Internet-of-Things, Embedded Systems, Robotics, Control System, Network and Communication, System Integration, as well as other topics in the field of Computer Engineering and Electrical Engineering. The Ultima Computing : Jurnal Sistem Komputer is published regularly twice a year (June and December) and is jointly managed by the Computer Engineering and Electrical Engineering Study Program at Universitas Multimedia Nusantara.

Call for Papers

International Journal of New Media Technology (IJNMT) is a scholarly open access, peer-reviewed, and interdisciplinary journal focusing on theories, methods and implementations of new media technology. Topics include, but not limited to digital technology for creative industry, infrastructure technology, computing communication and networking, signal and image processing, intelligent system, control and embedded system, mobile and web based system, and robotics. IJNMT is published twice a year by Faculty of Engineering and Informatics of Universitas Multimedia Nusantara in cooperation with UMN Press.

Ultimatics : Jurnal Teknik Informatika is the Journal of the Informatics Study Program at Universitas Multimedia Nusantara which presents scientific research articles in the fields of Analysis and Design of Algorithm, Software Engineering, System and Network security, as well as the latest theoretical and practical issues, including Ubiquitous and Mobile Computing, Artificial Intelligence and Machine Learning, Algorithm Theory, World Wide Web, Cryptography, as well as other topics in the field of Informatics.

Ultima Computing : Jurnal Sistem Komputer is a Journal of Computer Engineering Study Program, Universitas Multimedia Nusantara which presents scientific research articles in the field of Computer Engineering and Electrical Engineering as well as current theoretical and practical issues, including Edge Computing, Internet-of-Things, Embedded Systems, Robotics, Control System, Network and Communication, System Integration, as well as other topics in the field of Computer Engineering and Electrical Engineering.

Ultima InfoSys : Jurnal Ilmu Sistem Informasi is a Journal of Information Systems Study Program at Universitas Multimedia Nusantara which presents scientific research articles in the field of Information Systems, as well as the latest theoretical and practical issues, including database systems, management information systems, system analysis and development, system project management information, programming, mobile information system, and other topics related to Information Systems.

ISSN 2355-3286

FOREWORD

ULTIMA Greetings!

Ultima Computing : Jurnal Sistem Komputer is a Journal of Computer Engineering and Electrical Engineering at Multimedia Nusantara University which presents scientific research articles in the field of Computer Systems as well as the latest theoretical and practical issues, including Edge Computing, Internet-of-Things, Embedded Systems, Robotics, Control Systems, Network and Communication, System Integration, and other topics in the field of Computer Engineering and Electrical Engineering.

In this June 2023 edition, Ultima Computing enters the 1st Edition of Volume 15. In this edition there are six scientific papers from researchers, academics and practitioners in the fields of Computer Engineering and Electrical Engineering. Some of the topics raised in this journal are: Development of an Internet of Things-Based Garbage Collection Robot, Performance Comparison of YOLOv5 and YOLOv8 Architectures in Human Detection using Aerial Images, State-Feedback Control Design for the Cannon Stability System, Comparison of FIR and IIR Filters for Audio Signal Noise Reduction, Soil Moisture Control System for Lettuce Seeds: Time-based Alternative Approach and Simple and Accurate Instrumentation Device to Detect Loose-End Defective Cigarettes.

On this occasion we would also like to invite the participation of our dear readers, researchers, academics, and practitioners, in the field of Engineering and Informatics, to submit quality scientific papers to: International Journal of New Media Technology (IJNMT), Ultimatics : Jurnal Teknik Informatics, Ultima Infosys: Journal of Information Systems and Ultima Computing: Journal of Computer Systems. Information regarding writing guidelines and templates, as well as other related information can be obtained through the email address ultimacomputing@umn.ac.id and the web page of our Journal here.

Finally, we would like to thank all contributors to this June 2023 Edition of Ultima Computing. We hope that scientific articles from research in this journal can be useful and contribute to the development of research and science in Indonesia.

June 2023,

M.B.Nugraha, S.T., M.T.
Editor-in-Chief

ISSN 2355-3286

TABLE OF CONTENT

ISSN 2355-3286

Development of an Internet of Things-Based Garbage Collection Robot

Putri Liana[1], Rahmat Irsyada[2], Roihatur Rohmah[3]
[1] Department of Computer Systems, Faculty of Sains and Technology, Universitas Nahdlatul Ulama Sunan Giri, Bojonegoro, Indonesia
[1]putriliananew@gmail.com, [2]irsyada.rahmat@unugiri.ac.id, [3]roiha.rohmah@unugiri.ac.id

Accepted on 11 April 2022
Approved on 11 May 2023

***Abstract*— The problem of garbage is not a new thing from the past until now, garbage is still the center of attention and a prolonged problem because of the various impacts of the problems that are caused and felt. Many factors are the cause of the increasing amount of garbage every day, including the lack of self-awareness about maintaining cleanliness and disposing of garbage in its place. This study aims to develop an IoT-based garbage collection robot. The method in developing this garbage collection robot is using the Fuzzy Mamdani method. The IoT-based garbage collection robot is designed using the Arduino Uno microcontroller as well as the Node MCU ESP 8266, HC-SR04 sensor, DHT11 sensor, SG90 Servo motor, DC motor and L298N motor driver. The way this robot works is to detect the distance with the HC-SR04 sensor as a distance data input then processed by the Arduino microcontroller and then the SG90 servo motor will move to clamp the garbage automatically and for the robot using control via a smartphone to be directed to the destination garbage. The results of this study are that the robot can clamp or pick up garbage with a distance of less than 5 cm and can control the speed of a DC motor using the fuzzy Mamdani method.**

***Index Terms*— Arduino uno; Fuzzy Mamdani; HC-SR04 Sensor; Node MCU ESP8266; Garbage.**

I. INTRODUCTION

The garbage problem is not a new thing anymore from the past to the present, garbage is still the center of attention and a prolonged problem due to the various impacts of the problems caused and felt. There are many factors that cause the increasing amount of garbage every day, including the lack of awareness in oneself about maintaining cleanliness and throwing garbage in its place. Especially now that there is a Covid-19 pandemic that has hit the whole world, one of which is in Indonesia. The Indonesian government in stopping the pace of Covid-19 has also issued policies and statements in the form of work from home (WFH), Social distancing, Large Scale Social Restrictions (PSBB) and so on, which will affect the joints of people's lives[1].

During the Covid-19 pandemic, garbage can become very dangerous due to the nature of the virus that can last up to several days on inanimate objects [2]. Therefore, it is very important to be able to maintain the cleanliness of the environment by disposing of garbage in its place and also cleaning up scattered garbage to be able to avoid various impacts that occur, especially during the current pandemic, it can minimize the spread of the Covid-19 virus which can live in the inanimate object, one of which is garbage.

In the current era of the industrial revolution 4.0, technology plays an important role in everyday life. Technology is one of the needs and cannot be separated in all activities carried out, because technology makes all activities easier [2], faster, and also efficient [3]. Therefore, it is necessary to have new innovations created to be utilized and used in an effort to improve existing technological advances. In the use of technology to be able to facilitate work and also all activities carried out in the current era of revolution 4.0, robot technology continues to be developed. Developed countries such as Japan use robots to be able to help with human work [4]. Robots are made to facilitate human work which has been burdensome for some humans [5], [6].

Garbage problems can be overcome by utilizing technology, one of the efforts that continues to be carried out, one of which is by developing robot technology to be implemented as a garbage cleaning tool [7], [8]. In this study, an internet-based garbage collection robot of things will be developed which can be controlled via a smartphone, making it easier to clean up garbage and becoming one of the efforts to maintain environmental cleanliness during the Covid-19 pandemic.

II. RESEARCH MODELS AND METHODS

The method in this study used a waterfall model and used the fuzzy Mamdani method [9]. The stages in this method are planning, analysis, system design, design, and testing of results.

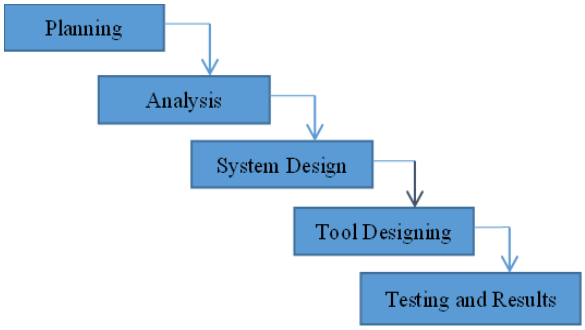

Figure 1. Waterfall model

A. *Planning*

Make plans related to how the performance and benefits of the system will be made. Planning various components of tools and materials that will be used in the manufacture of the Internet of Things-Based Garbage Collection Robot system where this robot will later use two microcontrollers that will control the system of this robot, namely the Arduino Uno microcontroller and also NodeMCu ESP 8266. For the development of this Internet of Things-Based Garbage Collector robot using the Fuzzy Mamdani Logic method.

In this planning stage, namely by analyzing the hardware needed in the development of IoT-based garbage collection robots, including:

- Arduino Uno
- NodeMCU Esp 8266
- Servo Motor
- DC motor
- Ultrasonic Sensors
- DHT 11 sensor
- L298N driver

The software needed in designing an internet of things-based garbage collection robot is :

- Arduino IDE for programming or coding microcontrollers
- Fritzing to design an electronic scheme for the manufacture of IoT-based garbage collection robots
- Matlab to determine the result of the calculation of the fuzzy Mamdani method

B. *Analysis*

Analyze how the robot works when the fuzzy Mamdani logic method is applied in regulating the speed of the DC motor. In analyzing the fuzzy Mamdani method where in this method there are two sensor inputs, namely the ultrasonic sensor and the DHT 11 sensor, it will then produce an output in the form of a DC motor rate velocity.

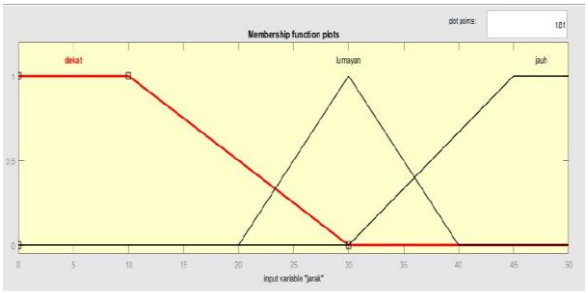

Figure 2. Distance Membership Function

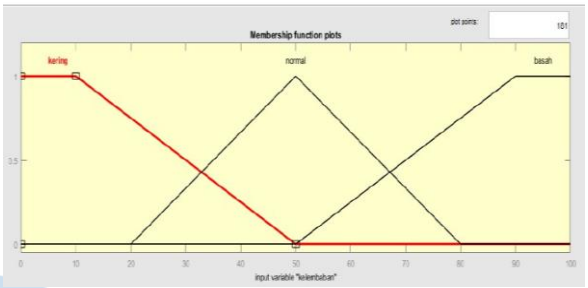

Figure 3. Moisture Membership Function

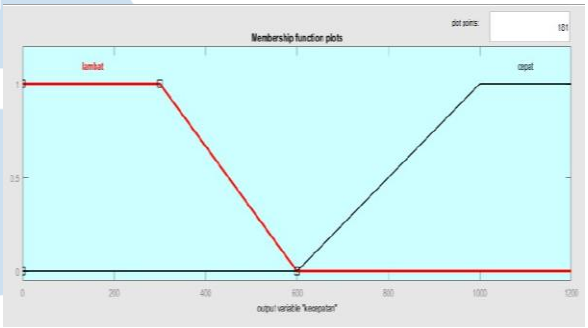

Figure 4. Speed Membership Function

Rules

- R1 : If Near And Wet Then Slow
- R2 : If Far And Normal Then slow
- R3 : If Not bad And dry then slow
- R4 : If Near And Dry Then Quickly
- R5 : If Far And Wet Then Fast
- R6 : If Not Bad And Normal Then Fast

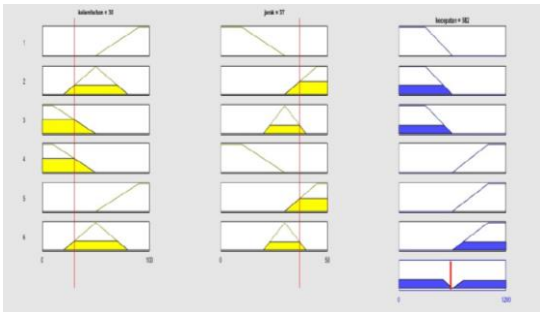

Figure 5. Fuzzy Mamdani Calculation

C. System Design

Designing how the system scheme will be made is by using a fritzing application. The fritzing application itself is widely used to design the design scheme of electronic devices to be made [10]. The following is the result of the design of the robot system using the Fritzing application.

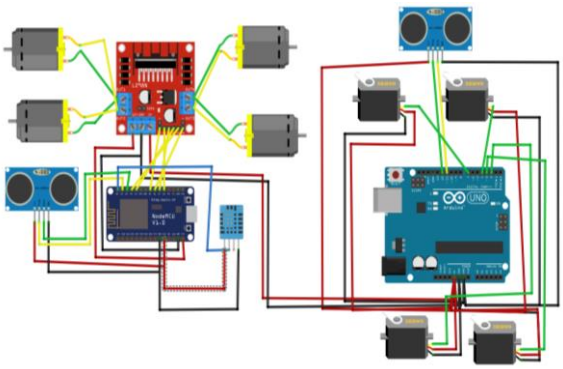

Figure 6. IoT-based Garbage Robot Circuit Schematic Design

From Fig. 6, it can be seen that the system design of the robot uses two microcontrollers, namely Arduino Uno and NodeMCU ESP 8266. There are four SG90 servos as a garbage stamping crust. L298N motor driver that regulates the speed of DC motors, ultrasonic sensors as a detection of obstacles [11] and also garbage, as well as a DHT 11 sensor to measure humidity [12] in the garbage box. Here is the flowchat system (Fig. 8) on the internet of things-based garbage collection robot.

In the garbage collection system, it uses a robotic arm system that functions to stamp garbage. The garbage collection arm uses a 4-servo motor crust that will move to stamp the garbage, while to detect the garbage using the HC-SR04 sensor. On the side of the robotic arm, a box is made that functions to hold the garbage that has been collected (Fig. 7).

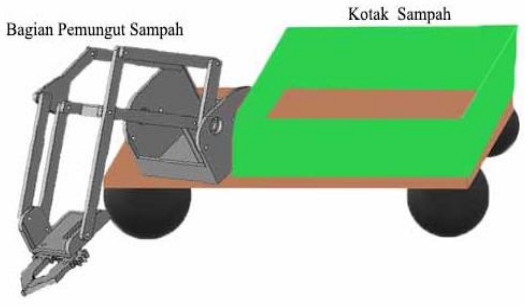

Figure 7. Prototype Design of IoT-Based Garbage Collection Robot

The design of the basic garbage collection robot uses boards to support various components of the garbage collection robot. For the crusting part, it uses 4 displaced wheels to walk the garbage collection robot to the garbage to be collected.

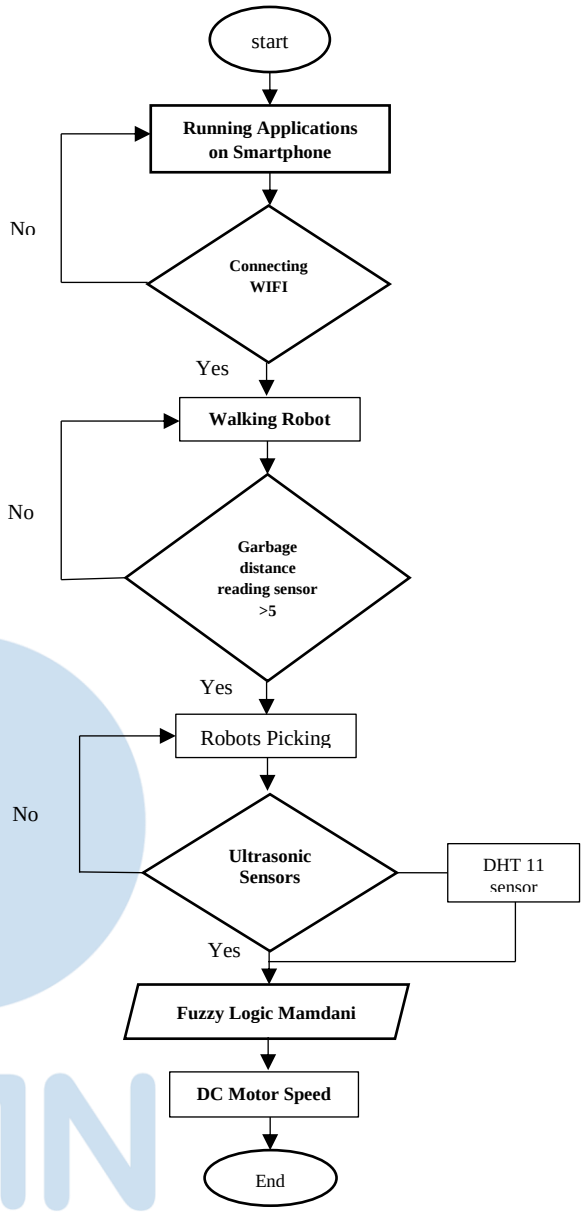

Figure 8. Robotic Flowchart

D. Tool Designing

Designing various components of the tool directly according to the design that has been made. Connects every pin present on the Node MCU Esp. 8266 component, Arduino UNO, HC-SR04 sensor, DHT 11 sensor and SG90 servo motor. In designing the tool, you must be careful to connect each pin on each component, because each pin on the electronic component has its own function.

Hardware design using a prototype model as follows:

- Ultrasonic sensor HC-SR04 as input detection [13] of objects or garbage to be collected
- Using a DC Motor as a wheel crust to run the robot system to the garbage to be collected

- Using the SG90 servo motor as a robotic arm crust that functions as a stamper and lifts the garbage to the garbage box
- Using ultrasonic sensors detects garbage capacity and to be able to regulate the speed of the running DC motor
- As well as a smartphone as a connector and controller of the direction of the running robot.
- DHT 11 sensor as a sandbox moisture counterh.

E. Testing and Results

Testing the IoT-based garbage collection robot that has been made whether it is in accordance with what is expected or needed. Then the results obtained from the experiment will be a reference on how the system works and the functioning of the system. For the due diligence plan of the IoT-based garbage collection robot work system using a scoring table based on user ratings. Furthermore, the results of the validation test assessment are calculated in the following way:

$$\text{percentage score} = \frac{\Sigma \text{ earned score}}{\Sigma \text{ maximum score}} \times 100\% \quad (1)$$

The percentage of score obtained is then measured using the score interpration for the Likert scale [14].

TABLE I. ELIGIBILITY CRITERIA GUIDELINES

Percentage	Interpretation
0%-25%	Very Unworthy
26%-50%	Not Worth It
51%-75%	Proper
76%-100%	Very Worthy

To be able to find out the response of users to develop IoT-based garbage collection robots, you can see from the likert scale table. From this likert scale, you can find out how the assessment of the work system from the robot can be used directly in cleaning up scattered garbage.

TABLE II. LINKERT ASSESSMENT SCALE

Criteria	Value
Less viable	1
Decent Enough	2
Proper	3
Very Worthy	4

III. RESULTS AND DISCUSSION

A. Results

This robot prototype is used to clean up scattered garbage, namely by stamping every garbage that you want to dispose of by being controlled through a smartphone then the HC SR04 ultrasonic sensor detects the object or garbage then automatically the robot picks up the garbage.

Figure 9. Prototype Robot Picking Up Garbage

In the garbage collection robot, the initial appearance of the robot runs using 4 DC motor wheels as a robotic speed booster [15]. As a series of robot supports, there is a rectangular acrylic as the base of the robot system. As a stamping system, it uses arm robots and ultrasonic sensors as inputs for detecting objects or garbage (Fig.10). On the left there is a garbage box as a place to collect garbage that has been collected.

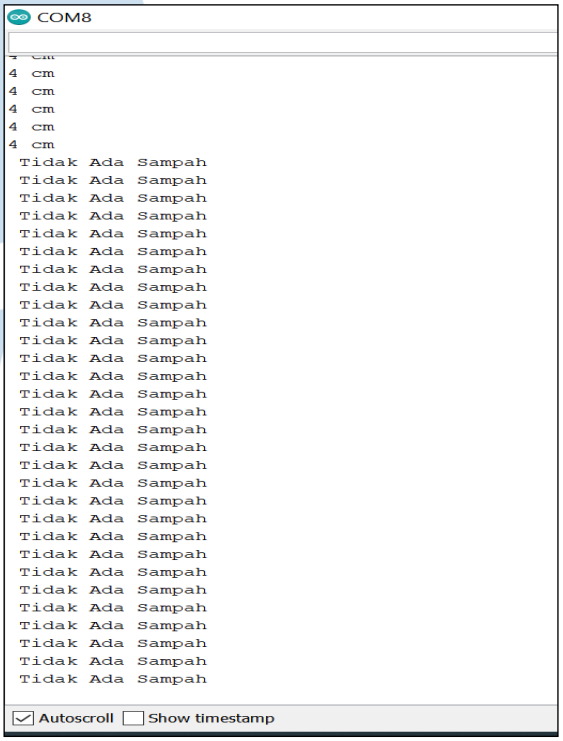

Figure 10. Ultrasonic Sensor Testing Monitor

At the testing stage, this tool aims to find out whether the system can pick up garbage that has been directed through an IoT-based smartphone, then the system picks up the garbage automatically through reading the distance of the garbage with the robot. The test results of this tool get the results in Table 3 and Table 4.

TABLE III. ULTRASONIC SENSOR TESTING

Testing	Distance (*cm*)	Garbage Detected
1	20	Undetectable Garbage
2	15	Undetectable Garbage
3	10	Undetectable Garbage
4	<5	Garbage Detected

TABLE IV. MAMDANI FUZZY TESTING

No	Humidity	Distance (*cm*)	DC Motor Speed
1	35	40	261
2	20	25	490
3	30	37	582
4	50	25	950
5	80	50	970

In testing the Fuzzy Mamdani method implemented in this IoT-based garbage collection robot (Fig. 11), it produces an output, namely the speed on the DC motor which will run quickly and slowly depending on the two inputs obtained from the ultrasonic sensor and the DHT11 sensor.

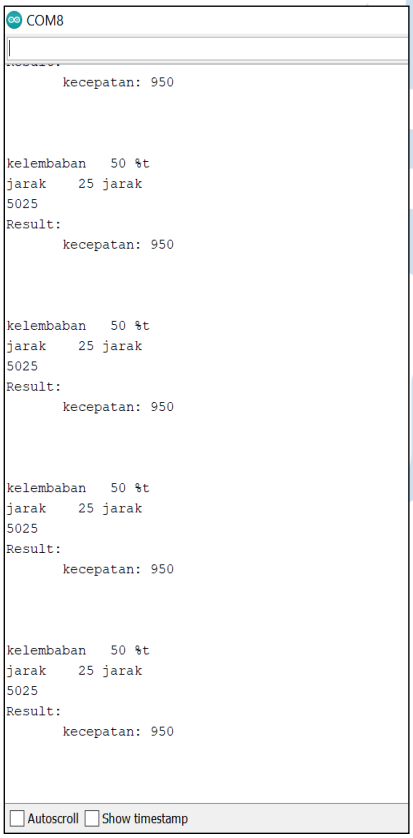

Figure 11. Serial Results of The Mamdani Fuzzy Test Monitor

B. *Discussions*

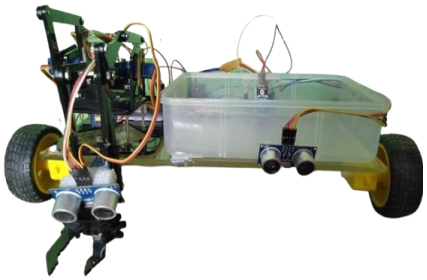

Figure 12. IoT-based Garbage Collection Robot

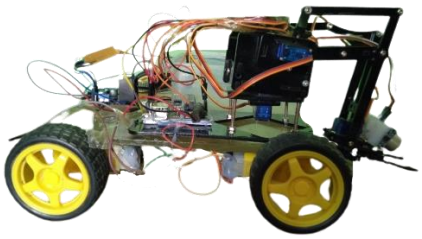

Figure 13. Robot View From The Side

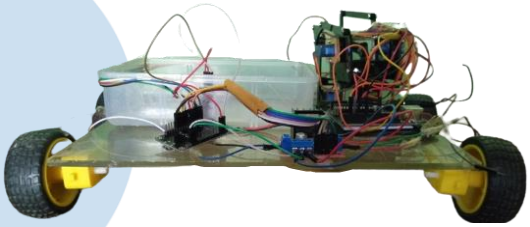

Figure 14. Robot View From Behind

This Internet of Things-based garbage collection robot is able to pick up garbage automatically with a garbage distance of less than 5 cm (Table 3). Then the garbage that has been collected is then put in the trash box. In the servo, the delay duration of each servo that moves to pick up garbage is set, which is for 5 seconds for a time lag for each servo movement. For the HC-SR 04 sensor as a garbage detector, the time is for 3 seconds every time it detects garbage. After the robot picks up and puts the garbage, then the robot will move to its original position to be able to pick up the detected garbage. Besides being able to pick up garbage, this robot can also detect various objects that you want to pick up or collect. This IoT-based garbage collection robot is able to pick up garbage with a load of up to 400 grams.

The method used in the development of iot-based garbage collection robots is the fuzzy Mamdani method, where there are 2 inputs [16], namely the ultasonic sensor and also the DHT 11 sensor and for the output, namely the speed of the DC motor [17]. The voltage used in this robot uses 2 lithium-ion batteries with a maximum voltage of 7200 mAh [18].

The feasibility test aims to find out how feasible the system of this internet of things-based garbage collection robot is to be used and utilized. In the feasibility test of this robot system, 6 respondents were

presented, including the principal of Klepek Islamic High School and Klepek Islamic High School Teacher. The results of feasibility testing can be seen in Table 5 of the Feasibility Test Results.

From the feasibility test in the table above, the prototype of this IoT-based garbage collection robot was calculated using a linker scale and got a result of 95.83%, which means it is very feasible.

TABLE V. DUE DILIGENCE RESULTS

No	Statement	Earned Score	Max Score	Percentage (%)	Category
1	Turn on the robot	24	24	100	Very Decent
2	Connecting a smartphone to the internet network	24	24	100	Very Decent
3	Controlling the robot using a smartphone	22	24	91,66	Very Decent
4	Picking up existing garbage	22	24	91,66	Very Decent
5	The appearance of the robot system is simple	23	24	95,83	Very Decent
6	Can pick up trash detected by sensors	23	24	95,83	Very Decent
7	Can run according to the controls on the smartphone	23	24	95,83	Very Decent
Earned Score		161			
Max Score			168		
Percentages and Categories				95,83	Very Decent

IV. CONCLUSIONS

The development of a garbage collection robot based on the Internet Of Things has been made with various electronic components namely arduino microcontroller, NodeMCU ESP 8266, ultrasonic sensors as well as DHT 11 sensors, L298N Motor Drivers, SG90 Servos, and also DC Motors. Ultrasonic sensor testing resulted in the sensor being able to detect garbage with a distance of less than 5 cm. For the method used in this IoT-based garbage collection robot using the fuzzy Mamdani method, which uses 2 inputs, namely the DHT 11 sensor and the ultrasonic sensor, it will then produce an output in the form of a speed of the DC motor on the Robot wheel.

ACKNOWLEDGMENT

The author would like to thank Nahdlatul Ulama Sunan Giri Bojonegoro University and also Klepek Islamic High School for facilitating the author in making this internet of things-based garbage collection robot in the task program at the end of the thesis.

REFERENCES

[1] M. W. P. Putra dan K. S. Kasmiarno, "Pengaruh Covid-19 Terhadap Kehidupan Masyarakat Indonesia: Sektor Pendidikan, Ekonomi Dan Spiritual Keagamaan," *POROS ONIM: Jurnal Sosial Keagamaan*, vol. 1, no. 2, hlm. 144–159, 2020, doi: 10.53491/porosonim.v1i2.41.

[2] R. Raja dan P. C. Nagasubramani, "Impact of modern technology in education," *Journal of Applied and Advanced Research*, vol. 3, no. 1, hlm. 33–35, 2018.

[3] E. Oztemel dan S. Gursev, "Literature review of Industry 4.0 and related technologies," *Journal of Intelligent Manufacturing*, vol. 31, no. 1, hlm. 127–182, 2020.

[4] L. Ellitan, "Competing in the era of industrial revolution 4.0 and society 5.0," *Jurnal Maksipreneur: Manajemen, Koperasi, dan Entrepreneurship*, vol. 10, no. 1, hlm. 1–12, 2020.

[5] I. A. Darmanto, "Inovasi Sistem Robotika Pada Perpustakaan," *JEECOM: Journal of Electrical Engineering and Computer*, vol. 2, no. 2, hlm. 13–16, 2020, doi: 10.33650/jeecom.v2i2.1185.

[6] S. Cooper, A. Di Fava, C. Vivas, L. Marchionni, dan F. Ferro, "ARI: The social assistive robot and companion," dalam *2020 29th IEEE International Conference on Robot and Human Interactive Communication (RO-MAN)*, 2020, hlm. 745–751.

[7] A. Jha, A. Singh, R. Kerketta, D. Prasad, K. Neelam, dan V. Nath, "Development of autonomous garbage collector robot," dalam *Proceedings of the Third International Conference on Microelectronics, Computing and Communication Systems*, 2019, hlm. 567–576.

[8] K. S. Kiran, P. Viswan, R. Joseph, P. Girish, dan S. Sreelekshmi, "GARBOT-THE GARBAGE COLLECTION ROBOT".

[9] M. A. Resources Information, *Fuzzy Systems: Concepts, Methodologies, Tools, and Applications: Concepts, Methodologies, Tools, and Applications*. IGI Global, 2017.

[10] T. Chen, L. Xu, dan K. Zhu, "FritzBot: A data-driven conversational agent for physical-computing system design," *International Journal of Human-Computer Studies*, vol. 155, hlm. 102699, 2021.

[11] J. Azeta, C. Bolu, D. Hinvi, dan A. A. Abioye, "Obstacle detection using ultrasonic sensor for a mobile robot," dalam *IOP Conference Series: Materials Science and Engineering*, 2019, vol. 707, no. 1, hlm. 012012.

[12] D. Srivastava, A. Kesarwani, dan S. Dubey, "Measurement of Temperature and Humidity by using Arduino Tool and DHT11," *International Research Journal of Engineering and Technology (IRJET)*, vol. 5, no. 12, hlm. 876–878, 2018.

[13] M. R. Hidayat, S. Sambasri, F. Fitriansyah, A. Charisma, dan H. R. Iskandar, "Soft water tank level monitoring system using ultrasonic HC-SR04 sensor based on ATMega 328 microcontroller," dalam *2019 IEEE 5th International Conference on Wireless and Telematics (ICWT)*, 2019, hlm. 1–4.

[14] E. L. Ardiyanti, A. S. Budi, dan I. M. Astra, "Pengembangan Ensiklopedia Alat Optik," *Prosiding Seminar Nasional Fisika*, vol. VII, no. 1, hlm. 9–15, 2018.

[15] M. Hijikata, R. Miyagusuku, dan K. Ozaki, "Wheel Arrangement of Four Omni Wheel Mobile Robot for Compactness," *Applied Sciences*, vol. 12, no. 12, hlm. 5798, 2022.

[16] H. M. Yasin *dkk.*, "IoT and ICT based smart water management, monitoring and controlling system: A review," *Asian Journal of Research in Computer Science*, vol. 8, no. 2, hlm. 42–56, 2021.

[17] A. K. Rajagiri, S. Rani, dan S. S. Nawaz, "Speed control of DC motor using fuzzy logic controller by PCI 6221 with MATLAB," dalam *E3S Web of Conferences*, 2019, vol. 87, hlm. 01004.
[18] J. Trevathan, S. Schmidtke, W. Read, T. Sharp, dan A. Sattar, "An IoT general-purpose sensor board for enabling remote aquatic environmental monitoring," *Internet of Things*, vol. 16, hlm. 100429, 2021.

ISSN 2355-3286

Performance Comparison of YOLOv5 and YOLOv8 Architectures in Human Detection Using Aerial Images

Indri Purwita Sary[1], Edmun Ucok Armin[2], Safrian Andromeda[3]
[1,2,3] Electrical Engineering, Universitas Singaperbangsa Karawang, Indonesia
[1] indripurwitasary@gmail.com, [2] edmun.ucok.armin@ft.unsika.ac.id, [3] safrian@ft.unsika.ac.id

Accepted on 10 June 2023
Approved on 30 June 2023

***Abstract*— The development of UAV technology has reached the stage of implementing artificial intelligence, control, and sensing. The use of cameras as UAV data inputs is being employed to ensure flight safety, search for missing persons, and disaster evacuation. Human detection using cameras while flying is the focus of this article. The application of human detection in pedestrian areas using aerial image data is used as the dataset in the deep learning input process. The architectures discussed in this study are YOLOv5 and YOLOv8. The precision, recall, and F1-score values are used as comparisons to evaluate the performance of these architectures. When both architecture performances are applied, YOLOv8 outperforms YOLOv5. The performance of the YOLOv8 model is greater than the YOLOv5 model for Precision, and F1-Score, the difference in the value of each performance is 2.82%, and 0.98%. As for the recall performance value, YOLOv5 is greater than the YOLOv8 model with a difference of 0.54%.**

***Index Terms*— Aerial Image; YOLOv5; YOLOv8; Precision; Recall; F1-Score.**

I. INTRODUCTION

Research on Unmanned Aerial Vehicles (UAVs) has made significant advancements recently. The latest progress in UAV development involves the implementation of artificial intelligence, control, and sensing technologies [1]. UAVs have been utilized by humans to aid in various tasks such as work assistance, surveillance, rescue operations, and security. Detecting humans from camera inputs on UAVs is a crucial task to ensure flight safety Furthermore, the utilization of UAVs in human search missions for safety purposes has also been developed [2]. An example of such utilization is security monitoring, where UAVs equipped with cameras are deployed for aerial surveillance to monitor environments or detect incidents [3]. In addition, detecting humans from UAV images is also used in search and rescue missions for locating and aiding missing or injured individuals in restricted areas [4]. Visual surveillance using UAV platforms has become fascinating. The majority of research works on visual data captured by UAVs are primarily focused on object detection and tracking tasks [5].

Introduction commonly contains the background, purpose of the research, problem identification, and research methodology conducted by the authors which been describe implicitly. Except for Introduction and Conclusion, other chapter's title must be explicitly represent the content of the chapter.

Research related to human object detection using cameras has been extensively conducted in recent years. Various situations are utilized to capture human images. A study on detecting non-rigid small-sized individuals at low altitudes using the VisDrone2019 dataset has been conducted by Xiang Qing Zhang et al., 2022[2]. This research utilized human images captured by cameras mounted on UAVs. The study focuses on improving object detection in complex backgrounds and poor lighting conditions. The DCLANet method employed in this research demonstrates the capability to detect non-rigid small-sized human objects in aerial images taken at low altitudes.

Garbage problems can be overcome by utilizing technology, one of the efforts that continues to be carried out, one of which is by developing robot technology to be implemented as a garbage cleaning tool [7], [8]. In this study, an internet-based garbage collection robot of things will be developed which can be controlled via a smartphone, making it easier to clean up garbage and becoming one of the efforts to maintain environmental cleanliness during the Covid-19 pandemicResearch on the use of YOLOv3 for tracking walking individuals and automatically capturing frontal photos was also conducted by Qifeng Shen in 2018 [6]. The data used in this study involved images captured by UAVs. The methods employed in this research included person detection and recognition using artificial neural networks within YOLOv3, Locality-constrained Linear Coding (LLC) method for face detection and localization, and vision-based UAV control. The results of the study demonstrated that the proposed methods were effective and practical for

tracking individuals and capturing frontal face images using UAVs.

Object detection of humans using aerial image data has also been conducted by Charalampos Symeonidis in 2022. The dataset used in this research is called AUTH-Persons. The dataset consists of videos of human crowds from an aerial perspective. The evaluation method for human object detection is referred to as NMS (Non-Maximum Suppression). This paper describes the dataset, its structure, and the methods used to evaluate the performance of three human detectors: Single Shot Detector (SSD), YOLOv3, and YOLOv4-tiny [1]. The results show that YOLOv3-512 (DarkNet53) achieves the best performance in terms of average precision (AP) at the intersection over union (IoU) thresholds of 0.5 and 0.95. The results also indicate that Seq2Seq-NMS outperforms other NMS methods in terms of AP at the 0.5 and 0.95 IoU thresholds. However, the paper notes that the shift in visual data distribution between training and testing samples can disproportionately negatively affect DNN-based NMS methods that exploit appearance-based features compared to those that do not.

Research on object detection and classification with Unmanned Aerial Vehicles (UAVs) using machine learning algorithms has been conducted. This study compares the performance of two architecture versions, namely YOLOv3 and YOLOv5, for object detection in UAV images. In 2022, Teddy Surya Gunawan utilized data preparation, model training, and implementation methods. The research results demonstrate that the YOLOv5 architecture outperforms YOLOv3 in object detection and classification in UAV images [7].

Research on human detection using two camera data, namely thermal imaging camera and images from a UAV camera, was conducted by Jewel Kate D in 2022. The data collected was processed through a neural network to identify whether the object is a human, and the YOLOv5 algorithm was used to classify the detected objects by the drone. This research utilized the CoCo dataset for the training process and evaluated the accuracy of the device by determining the number of humans detected by the device at various distances and comparing it with the actual number of humans. The research results demonstrate that the device is capable of detecting humans and achieving a low error percentage [8].

Jun-Hwa Kim has implemented YOLOv8 in his research. The YOLOv8 architecture is used to detect drones and birds. This architecture is employed to differentiate between drones and birds. Testing of aerial bird and drone images was conducted using 77 videos. The training results were then used to evaluate 30 video images over 93 epochs. The evaluation metric used was Average Precision (AP) for each test video, with detections considered correct if the Intersection over Union (IoU) with the ground truth box was above 0.5. The frame per second (FPS) of the P2 layer and Multi-Scale Image Fusion (MSIF) with the YOLO-V8-M model were 45.7 fps and 17.6 fps, respectively, for image sizes of 640 and 1280 [9].

Detecting human objects is commonly used as input in various UAV missions. Therefore, the author chose human detection as the object of interest in aerial images. The YOLO architecture has multiple versions, and YOLOv8 is the latest architecture to be used in the testing. Based on previous research, the YOLOv5 architecture has been tested for human detection. Hence, the performance of the YOLOv5 and YOLOv8 architectures will be compared in detecting humans in aerial images.

II. METHODS

The method used in this research is deep learning using the YOLOv5 and YOLOv8 architectures. Deep learning will be applied to human images in pedestrian scenarios. This study focuses on comparing the performance of both architectures.

A. YOLOv5

There have been changes to the standard architecture of model arrangement in YOLOv5. The model arrangement is now divided into three components: backbone, neck, and head. The backbone of YOLOv5 is Darknet 53. Darknet 53 is a new network architecture that focuses on feature extraction characterized by small filter windows and residual connections [10]. The neck of YOLOv5 acts as a connector between the backbone and the head. The neck of YOLOv5 functions to gather and refine the features extracted by the backbone, with a focus on enhancing spatial and semantic information at various scales [11]. The head of YOLOv5 consists of three branches, each predicting features at different scales. Each head produces bounding boxes, class probabilities, and confidence scores. Finally, the network uses Non-maximum Suppression (NMS) to filter overlapping bounding boxes [11].

B. YOLOv8

YOLOv8 is the latest version of the object detection model architecture, succeeding YOLOv5. YOLOv8 introduces improvements in the form of a new neural network architecture [11]. Two neural networks are implemented, namely the Feature Pyramid Network (FPN) and the Path Aggregation Network (PAN), along with a new labeling tool that simplifies the annotation process. This labeling tool contains several useful features, such as automatic labeling, shortcut labeling, and customizable hotkeys. The combination of these features makes it easier to annotate images for training the model.

FPN works by gradually reducing the spatial resolution of the input image while increasing the number of feature channels. This results in the creation

of a feature map that is capable of detecting objects at different scales and resolutions. On the other hand, the PAN architecture can combine features from different network levels through skip connections. Consequently, the network can capture features more effectively at various scales and resolutions, which is crucial for accurately detecting objects of different sizes and shapes [12].

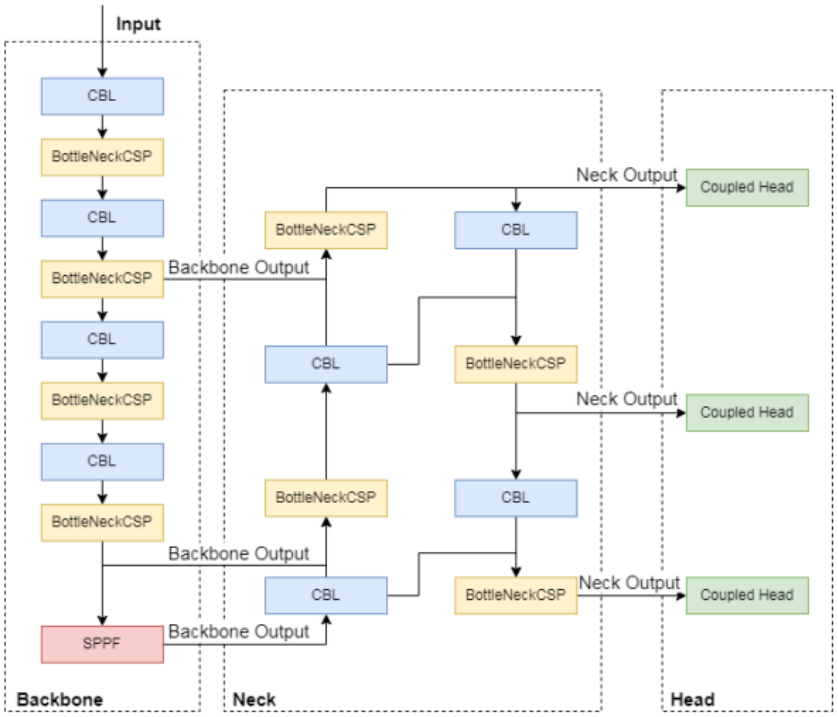

Figure 1. The structure of YOLOv5 [12]

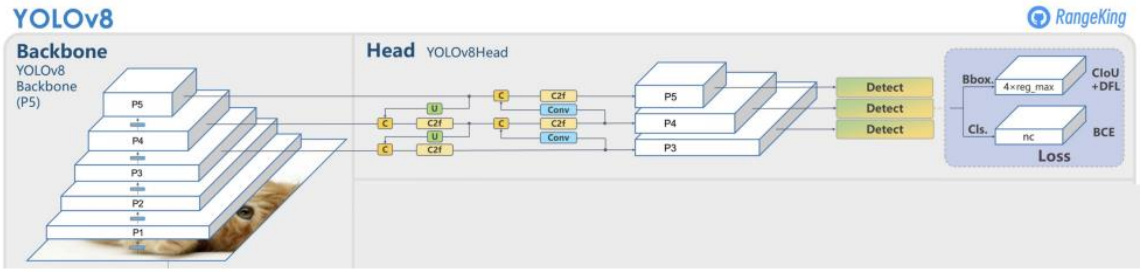

Figure 2. YOLOv8 Architecture[10]

C. *Evaluation Metrics*

Confusion matrix is used to evaluate the performance of a machine learning model. The confusion matrix is a matrix that displays the predictions of the actual classification and the predicted classification [13]. There are four classifications in the confusion matrix, namely True Negative (TN), True Positive (TP), False Negative (FN), and False Positive (FP) derived from actual and predicted values. The definitions of the confusion matrix are shown in Table 4, where TP (True Positive) is the number of positive samples correctly classified; TN (True Negative) is the number of negative samples correctly classified; FP (False Positive) is the number of negative samples wrongly classified as positive; FN (False Negative) is the number of positive samples wrongly classified as negative [14]. An illustration of the confusion matrix can be seen in Figure 2. The model's performance can be calculated using precision, recall, and F1-score derived from the confusion matrix.

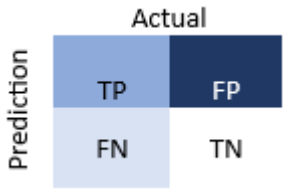

Figure 3. Confusion Matrix

Precision is the ratio of TP to the total number of predicted positive data. In the denominator, there is the variable FP as the divisor. This can be written using Equation 1[15].

$$\text{precision} = \frac{\text{TP}}{\text{TP+FP}} \quad (1)$$

On the other hand, recall is defined as the ratio of TP to the total number of actually positive instances. The denominator includes FN as the divisor, and it can be written using Equation 2[15].

$$\text{recall} = \frac{\text{TP}}{\text{TP+FN}} \quad (2)$$

When recall is very high, precision will be very low, and vice versa. There is a trade-off relationship between precision and recall. This trade-off relationship implies that the sum of these two variables equals 1. The harmonization of the average between precision and recall is called the F1-score. Based on Equation 3[15], the best value for the F1-score is 1.0, while the worst value is 0.0.

$$\text{F1} = \frac{2\times\text{precision}\times\text{recall}}{\text{precision+recall}} \quad (3)$$

III. Results and Discussion

The aerial image data used in this paper is the pedestrian dataset from Roboflow. The dataset from https://universe.roboflow.com/edmundpub/pedestrian aerial. Our research used google collab for training and validate the model with 100th epoch. 828 aerial images were used in training the YOLOv5 and YOLOv8 for human detection. The models were validated using 233 aerial images in human detection.

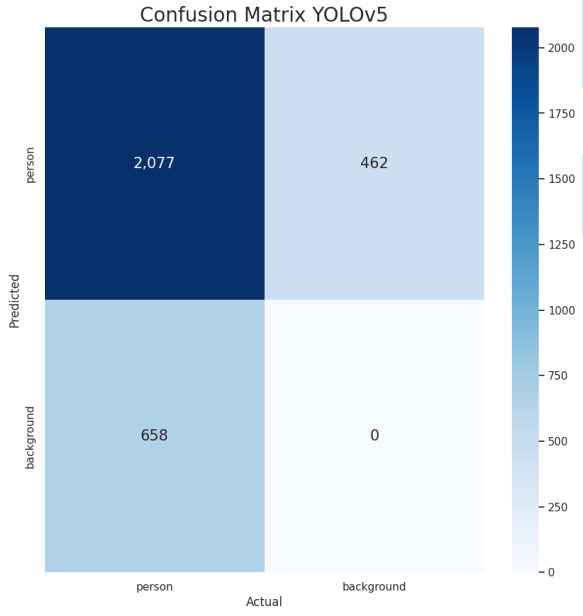

Figure 4. Confusion Matrix YOLOv5

The confusion matrix of YOLOv5 at the last epoch can be seen in Figure 4. The values of TP 2077, FP 463, and FN 658. The number of each value become from detected the human in aerial image from validation stage. Based on Eq.1, the precision value at the last epoch is 0.8177 or 81.77%. Recall value based on Equation 2 is 0.7594 or 75.41%. F1-score results obtained with Eq.3 are 0.7876 or 78.76%. These performance results are summarized in Table 1. While the precision, recall, and F1-Score values for each epoch are illustrated in Fig.6.

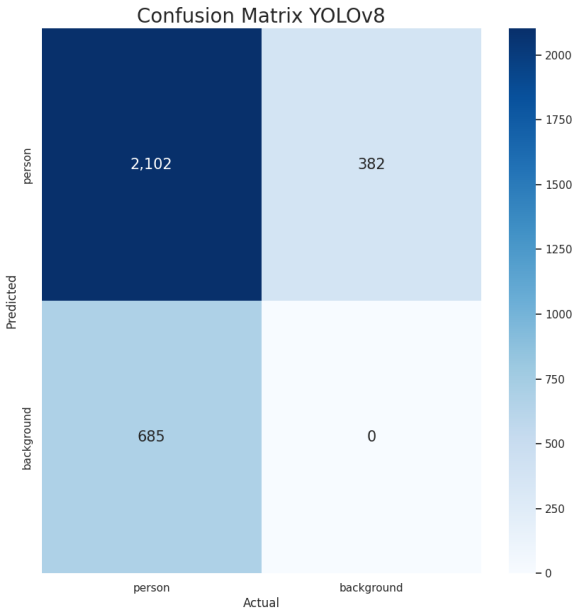

Figure 5. Confusion Matrix YOLOv8

The confusion matrix on YOLOv8 at the last epoch can be seen in Figure 5. TP values are 2102, FP 382, and FN 685. Based on Equation 1, the precission value at the last epoch is 0.8462 or 84.62%. Recall value based on Equation 2 is 0.7540 or 75.40%. F1-score results obtained with Equation 3 are 0.7998 or 79.98%. these performance results are summarized in Table 1. While the precision, recall, and F1-Score values for each epoch are illustrated in Fig 7.

TABLE I. YOLOV5 AND YOLOV8 MODEL PERFORMANCE

Architecture	Precision	Recall	F1-Score
YOLOv5	0.8180	0.7594	0.7876
YOLOv8	0.8462	0.7540	0.7974

The performance values of the YOLOv5 and YOLOv8 models are summarized in Table 1. The YOLOv8 model is 0.0282 or 2.82% larger than YOLOv5 for the precision value. The difference in the recall value of the YOLOv5 model is greater than that of YOLOv8 which is 0.0054 or 0.54%. The F1-score value of the YOLOv8 model is greater than that of YOLOv5 by 0.0098 or 0.98%.

The performance results of precision, Recall, and F1-score in graphical form can be seen in Fig.6 and Fig.7. The performance values for the YOLOv5 and YOLOv8 model graphs are known to increase until the last epoch. From the characteristics of the graphs in Figure 7 and Figure 8, it can be seen that the training process does not occur overfitting and underfitting. This shows that the learning process of deep learning has run without any problems.

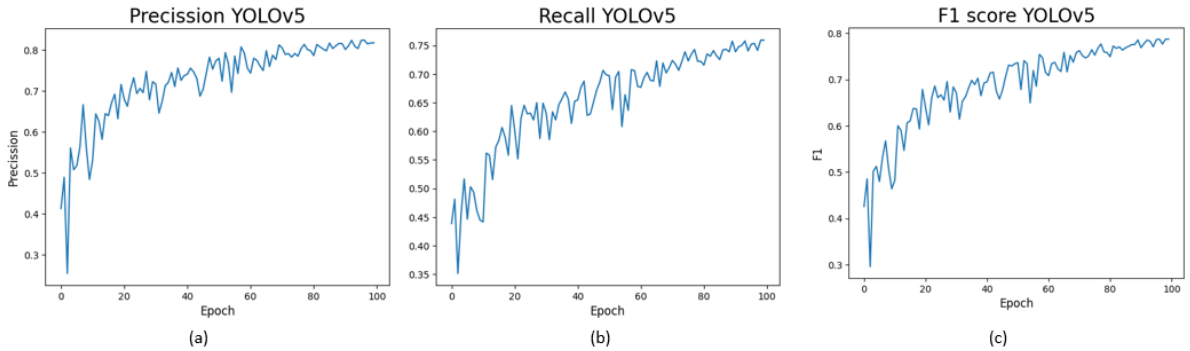

Figure 6. YOLOv5 Performance Results

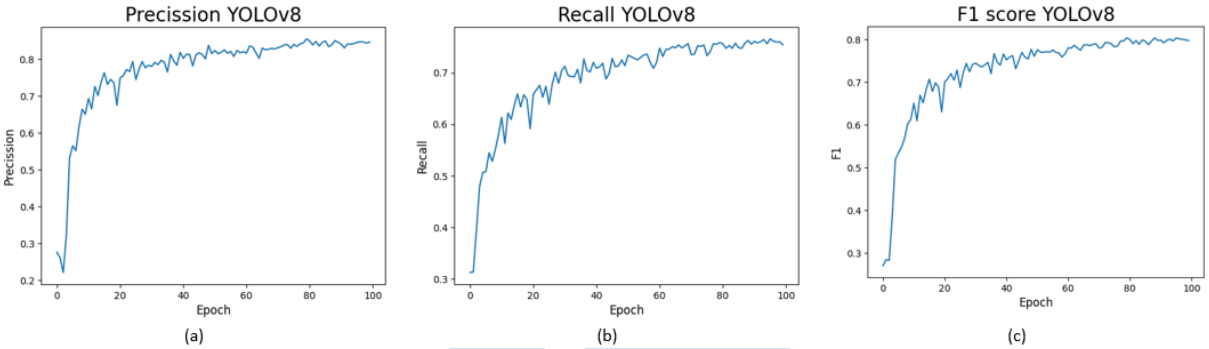

Figure 7. YOLOv8 Performance Results

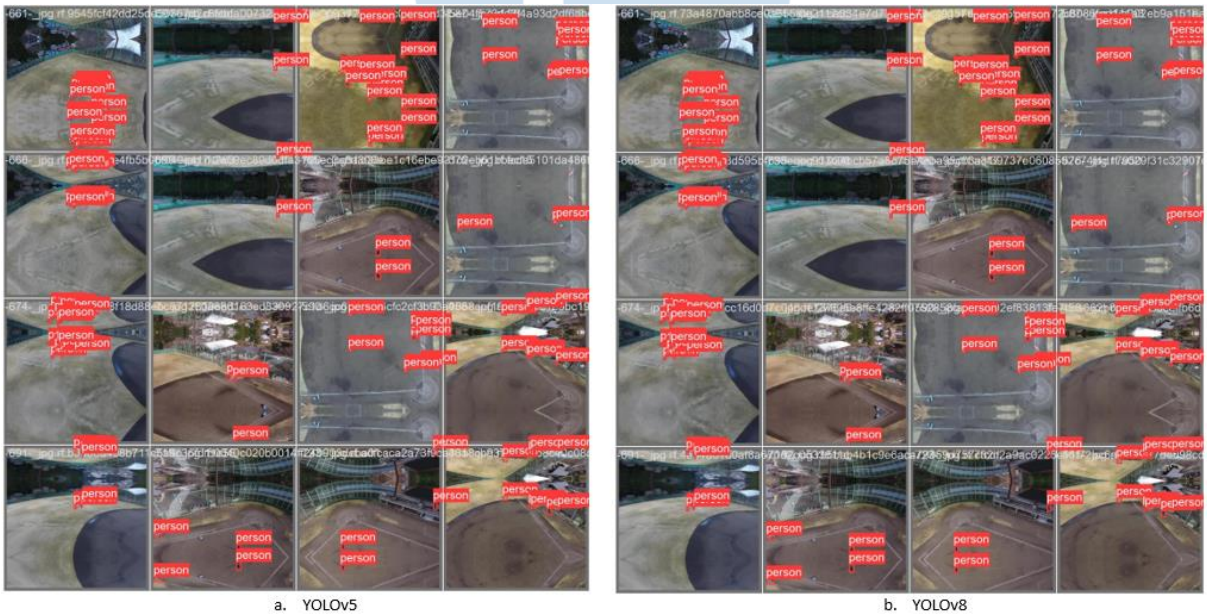

Figure 8. Human Detection Results

The results of aerial image training that has been applied to the YOLOv5 and YOLOv8 models can be seen in Figure 8. The person label in Figure 8 is the result of human detection. Both images show that the YOLOv5 and YOLOv8 models have successfully detected humans.

IV. CONCLUSIONS

Based on the research results discussed, it is known that the YOLOv5 and YOLOv8 models have successfully detected humans in aerial images. There are differences in performance values in human detection. The performance value of the YOLOv8 model is greater than the YOLOv5 model for precision and F1-score, the difference in the value of each performance is 2.82%, and 0.98%. As for the recall performance value, YOLOv5 is greater than the YOLOv8 model with a difference of 0.54%.

REFERENCES

[1] C. Symeonidis, I. Mademlis, I. Pitas, and N. Nikolaidis, "AUTH-PERSONS: A DATASET FOR DETECTING HUMANS IN CROWDS FROM AERIAL VIEWS," in Proceedings - International Conference on Image Processing, ICIP, IEEE Computer Society, 2022, pp. 596–600. doi: 10.1109/ICIP46576.2022.9897612.

[2] X. Zhang, Y. Feng, S. Zhang, N. Wang, and S. Mei, "Finding Nonrigid Tiny Person With Densely Cropped and Local Attention Object Detector Networks in Low-Altitude Aerial Images," IEEE J Sel Top Appl Earth Obs Remote Sens, vol. 15, pp. 4371–4385, 2022, doi: 10.1109/JSTARS.2022.3175498.

[3] H. Ugochi Dike, Q. Wu, Y. Zhou, and G. Liang, "Unmanned Aerial Vehicle (UAV) Based Running Person Detection from a Real-Time Moving Camera," in Proceedings of the 2018 IEEE International Conference on Robotics and Biomimetics, IEEE, 2018, pp. 2273–2278.

[4] A. G. Popa, L. Ichim, and D. Popescu, "Real-time person detection from UAV images using performant neural networks," in 2022 14th International Conference on Electronics, Computers and Artificial Intelligence, ECAI 2022, Institute of Electrical and Electronics Engineers Inc., 2022. doi: 10.1109/ECAI54874.2022.9847477.

[5] S. Zhang et al., "Person Re-Identification in Aerial Imagery," IEEE Trans Multimedia, vol. 23, pp. 281–291, 2021, doi: 10.1109/TMM.2020.2977528.

[6] Q. Shen, L. Jiang, and H. Xiong, "Person Tracking and Frontal Face Capture with UAV," in 2018 18th IEEE International Conference on Communication Technology, IEEE, 2018, pp. 1412–1416.

[7] T. S. Gunawan, I. M. M. Ismail, M. Kartiwi, and N. Ismail, "Performance Comparison of Various YOLO Architectures on Object Detection of UAV Images," in 8th IEEE International Conference on Smart Instrumentation, Measurement and Applications, ICSIMA 2022, Institute of Electrical and Electronics Engineers Inc., 2022, pp. 257–261. doi: 10.1109/ICSIMA55652.2022.9928938.

[8] J. K. D. Lagman, A. B. Evangelista, and C. C. Paglinawan, "Unmanned Aerial Vehicle with Human Detection and People Counter Using YOLO v5 and Thermal Camera for Search Operations," in 2022 IEEE International Conference on Automatic Control and Intelligent Systems, I2CACIS 2022 - Proceedings, Institute of Electrical and Electronics Engineers Inc., 2022, pp. 113–118. doi: 10.1109/I2CACIS54679.2022.9815490.

[9] J.-H. Kim, N. Kim, and C. S. Won, "High-Speed Drone Detection Based On Yolo-V8," in ICASSP 2023 - 2023 IEEE International Conference on Acoustics, Speech and Signal Processing (ICASSP), IEEE, Jun. 2023, pp. 1–2. doi: 10.1109/ICASSP49357.2023.10095516.

[10] D. Reis, J. Kupec, J. Hong, and A. Daoudi, "Real-Time Flying Object Detection with YOLOv8," ArXiv, vol. 1, no. 2305.09972, May 2023, [Online]. Available: http://arxiv.org/abs/2305.09972

[11] J. Terven and D. Cordova-Esparza, "A Comprehensive Review of YOLO: From YOLOv1 and Beyond," ACM Comput Surv, Apr. 2023, [Online]. Available: http://arxiv.org/abs/2304.00501

[12] H. Liang, J. Chen, W. Xie, X. Yu, and W. Wu, "Defect detection of injection-molded parts based on improved-YOLOv5," in Journal of Physics: Conference Series, Institute of Physics, 2022. doi: 10.1088/1742-6596/2390/1/012049.

[13] G. Zeng, "On the confusion matrix in credit scoring and its analytical properties," Commun Stat Theory Methods, vol. 49, no. 9, pp. 2080–2093, May 2020, doi: 10.1080/03610926.2019.1568485.

[14] Y. Zhang, T. Zuo, L. Fang, J. Li, and Z. Xing, "An Improved MAHAKIL Oversampling Method for Imbalanced Dataset Classification," IEEE Access, vol. 9, pp. 16030–16040, 2021, doi: 10.1109/ACCESS.2020.3047741.

[15] Z. Ning, X. Wu, J. Yang, and Y. Yang, "MT-YOLOv5: Mobile terminal table detection model based on YOLOv5," in Journal of Physics: Conference Series, IOP Publishing Ltd, Jul. 2021. doi: 10.1088/1742-6596/1978/1/012010.

ISSN 2355-3286

State-Feedback Control Design for the Cannon Stability System on Tank

Ahmad Syahril Muharom
Electrical Engineering, Universitas Multimedia Nusantara, Tangerang, Indonesia
ahmad.syahril@umn.ac.id

Accepted on 14 June 2023
Approved on 30 June 2023

***Abstract*— Tanks have an important role in protecting a region in the event of a battle. The tank's cannon is a very reliable weapon in warfare. However, the cannon's precision while aiming and firing targets is a concern. A control system must be created to increase the cannon's stability and precision. The state feedback control technique with a full-state observer is the control system that can manage cannon disturbances. The control system is built around three DC motors, each of which operates the cannon's x, y, and z axes. Then performed tests for each axis at an angle of 90 degrees, The state feedback control with a full state observer can produce outstanding performance, with the time required for the cannon to reach the target angle was 0.51 seconds, and the cannon system had 0% overshoot.**

***Index Terms*—Cannon; Full-state Observer; State Feedback Control; Tank.**

I. INTRODUCTION

A country needs military vehicles that are used as instruments to protect or destroy threats [1][2], The main weapon of the tank will be unstable as it tries to cross different heights. Stability is something that must be considered, the cannon must be stable so that the tank can shoot its target accurately [3].

PID control is a traditional control method, is one of many that can be used to stabilize a cannon tank. This traditional control mechanism works well to control oscillations in the system and can be utilized for stability [4].

This system also has many problems, such as being non-linear, poorly actuated, and complex. To improve system performance, researchers are interested in creating this system. State feedback controllers are one of the control strategies utilized to manage this tank cannon system [5]. To describe all states in the cannon tank system, a state feedback controller is not sufficient [6]. To know every state in this system, a state observer must be added [7]. In this study, state feedback control with a full-state observer is used to regulate the cannon tank system. By determining the desired pole, the full-state observer parameter and gain observer are added using the pole placement method. The decision is taken in order to achieve the best reaction with the least amount of control signal..

II. SYSTEM MODELLING

A. Transfer Function DC Servo Motor

This research on the cannon tank aims to control the entire position of the cannon, the actuator uses DC servo motors for each x, y and z-axis [8]. The design of the cannon tank shown in Fig. 1.

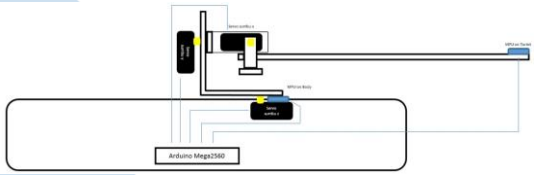

Figure 1. Design of Cannon Tank

The equivalent DC servo motor circuit can be seen in Fig. 2.

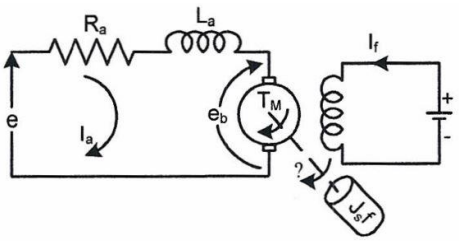

Figure 2. Equivalent Circuit of DC Servo Motor

The transfer function of the servo system can be written as:

$$\frac{\theta(s)}{Ea(s)} = \frac{Ktn}{s[LaJs^2+(Laf+RaJ)s+Raf+KtnKb]} \quad (1)$$

Where,
Ra = Armature Resistor (2.5 Ω)
La = Armature Inductance (0.062 H)
Ia = Armature Current
Va = Applied Armature Voltage
τ = Motor Torque
J = Motor Moment of Inertia (0.00004 Kg/m^2)
Ktn = Motor torque constant 0.026 (Nm/A)
Kb = Back EMF Constant 0.02 ($v.s\ /rad$)

Considering the value of the gear ratio and the torque of each servo [9], the torque equation for the servo is:

$$T_{total} = (T_m \times n) + t_{disturbance} \quad (2)$$

where n is the gear ratio. Then the block diagram changes to:

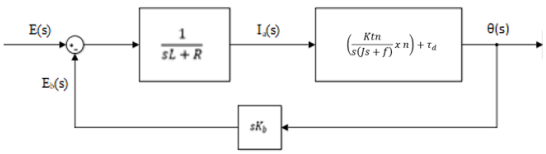

Figure 3. Servo Block Diagram with Gear Ratio and Torque Disturbance

Using the block diagram in Fig. 3, the transfer function for servo x, servo y, and servo z is found:

$$TF_{\text{servo x}} = \frac{0.000003234s^2+0.00008085s+0.117}{0.000002545s^3+0.0001636s^2+0.00484s} \quad (3)$$

$$TF_{\text{servo y}} = \frac{0.0000008154s^2+0.00002038s+0.117}{0.000002486s^3+0.0001624s^2+0.00484s} \quad (4)$$

$$TF_{\text{servo z}} = \frac{0.000005272s^2+0.0001318s+0.117}{0.000002585s^3+0.0001646s^2+0.00484s} \quad (5)$$

B. State Space Representation

The system is shown in a state space model in Figure 4.

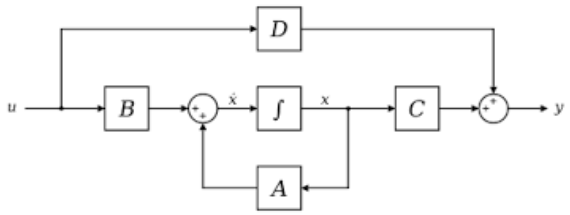

Figure 4. Open-Loop System Representation In State Space

The representatives of the state space equation can be derived as [10].

$$x = Ax + Bu \quad (6)$$

$$y = Cx + Du \quad (7)$$

Determine all coefficients in the numerator and denominator of a transfer function by expanding it [11]. This should result in the following form:

$$G(s) = \frac{n_1s^3+n_2s^2+n_3s+n_4}{s^4+d_1s^3+d_2s^2+d_3s+d_4} \quad (8)$$

The following method can now be used to directly insert the coefficients into the state-space model [12]:

$$\dot{x}(t) = \begin{bmatrix} 0 & 1 & 0 & 0 \\ 0 & 0 & 1 & 0 \\ 0 & 0 & 0 & 1 \\ -d_4 & -d_3 & -d_2 & -d_1 \end{bmatrix} x(t) + \begin{bmatrix} 0 \\ 0 \\ 0 \\ 1 \end{bmatrix} u(t)$$

$$y(t) = [n_4 \quad n_3 \quad n_2 \quad n_1]x(t)$$

.

III. State Feedback Control Design

A. State Feedback Controller

A state feedback control system can be seen in Fig. 5 as a diagram. The closed-loop eigenvalues are placed at the desired location using the feedback gain K in state feedback control. To get the output of the system to track the target location despite disturbances is the goal of the feedback control [13].

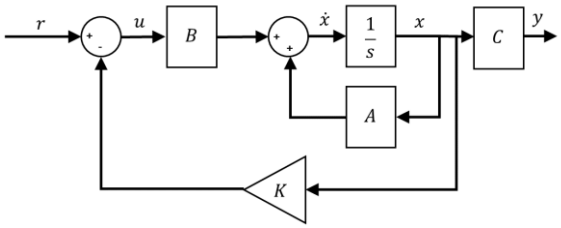

Figure 5. Closed-loop in State Space

The state feedback control system's dynamic equation is obtained.

$$\dot{x} = (A - BK)x + Bu \quad (9)$$

$$y = Cx \quad (10)$$

$$u = r - Kx \quad (11)$$

Before implementing the controller, the system model must be analyzed for controllability and observability. The system is controllable if and only if the controllability matrix in Equation (12) has rank=n, where n is the size of the system order [14].

$$C = [B|AB|A^2B| \ldots |A^{j-1}B] \quad (12)$$

Equation (13) is the observability matrix, and the system is observable if and only if the matrix has rank=n.

$$O = [C|CA|CA^2| \ldots |CA^{j-1}] \quad (13)$$

The closed loop's transfer function H(s) has a gain N, 0<N<1, for a unit-step reference input. The closed loop system in Fig. 4 is shown with a transfer function and is given as:

$$H(s) = C\big(sI - (A - BK)\big)^{-1}B \quad (14)$$

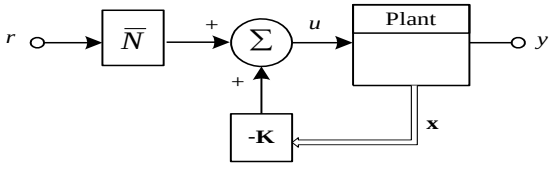

Figure 6. Closed-loop system with gain

The equation of state space can be derived as follow:

$$\dot{x} = (A - BK)x + Bu \quad (15)$$

$$y = Cx \quad (16)$$

$$u = r\bar{N} - Kx$$

$$\begin{bmatrix} N_x \\ N_u \end{bmatrix} = \begin{bmatrix} A & B \\ C & D \end{bmatrix}^{-1} \begin{bmatrix} 0 \\ 1 \end{bmatrix}$$

$$\bar{N} = N_u - KN_x \quad (17)$$

B. Controller Design by Pole Placement

A technique based on complete state feedback control is the pole placement, as shown in Fig. 5. The denominator of the closed-loop system in Fig. 4 can be determined using the Laplace transfer function [15]. The control gain K can be found by minimizing the performance function.

$$D(s) = sI - (A - BK) \quad (18)$$

I is the identity matrix in this case. As a result, all of the eigenvalues of **(A-BK)** can be used to assess the stability and transient response characteristics of the closed-loop system. The decision to use a feedback gain design is an attempt to K such that the eigenvalues of **(A-BK)** have negative real values [16].

C. Full State Observer

The observer has a few ways to derive its equation of state from the actual equations of the system, which are in the form of Equations (6) and (7). The full-state observer is shown in Fig. 7.

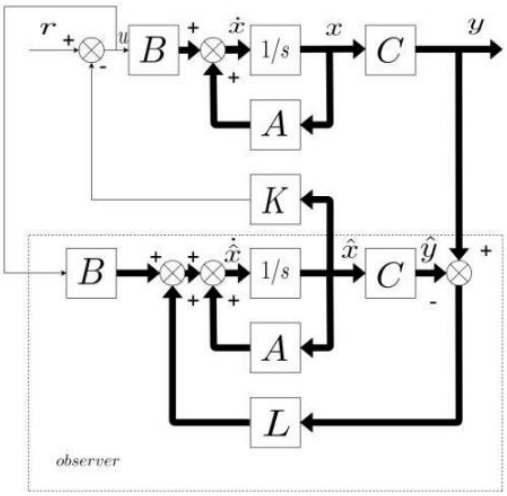

Figure 7. Closed-loop system with Full-State Observer

The gain observer is represented by Equation (18), where L is a n x m matrix. With the original state **x(t)** substituted by the estimate **x̂(t)** and the difference between the actual measured output **y(t)** and the estimate **ŷ(t)**, respectively, the state equations in Equations (18) and (19) model the true equations of the system [17].

$$\dot{\hat{x}} = A\hat{x} + Bu + L(y - \hat{y}) \quad (19)$$

$$\hat{y} = C\hat{x} \quad (20)$$

Substituting the equation **ŷ(t)** into the state equation of the observer will result in an alternative form for the model observer as in Equation (20).

$$\dot{\hat{x}} = (Ax + Bu) - \left(A\hat{x} + Bu + L(Cx - C\hat{x})\right) \quad (21)$$

IV. Results and Discussion

A. Controller Specifications

In this research, it is desired that the maximum overshoot be below 5% and the maximum rise time be 1 second. From these parameters, the values of **ωn** and **ζ** are obtained as 1.8 and 0.7, respectively. Then, to determine the control pole, see Fig. 8.

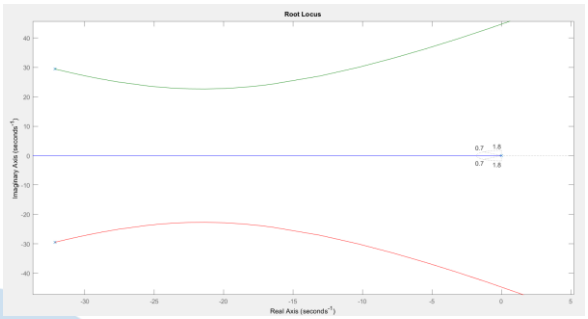

Figure 8. Root Locus Diagram of An Uncompensated System

In Fig. 9, there are values of **ζ** and **ωn** in the uncontrolled system. To determine the pole placement based on the specifications, the poles need to be placed inside the angle formed from the imaginary axis 0.7 (inside the sloping line of approximately 45 degrees) to realize the specification of overshoot below 5%. To realize a rise time of less than 1 second, the poles should be placed outside the half circle around 0.7 and 1.8.

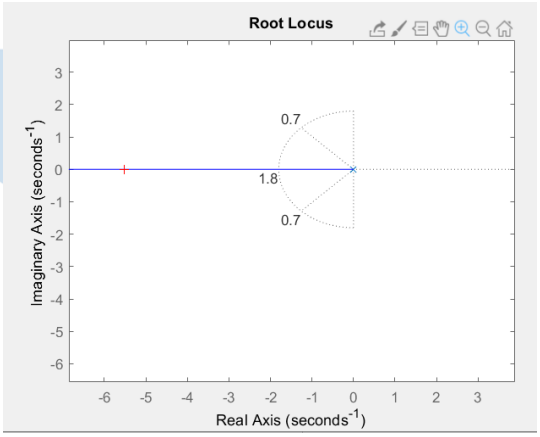

Figure 9. Pole Placement Control In The Root Locus

B. Observer Specifications

The observer desired to estimate ten times faster. Therefore, the pole location of the observer has a value ten times that of the controller's poles. Using equation (20), the gain of the observer is obtained as follows:

L1= 107.06

L2= 3.25

L3= 0.01

C. *State-Feedback Control with A Full-State Observer*

State-Feedback Control with a Full-State Observer Design is used to control the y servo contributing to roll, the x servo for pitch, and the z servo for yaw. Before implementation on the cannon, simulation is required to ensure the control system design is good and correct. Based on Fig. 5, the closed loop system has a gain value K as follows:

K1 = 0.0004

K2 = -0.0305

K3 = 5.98

The value is obtained by **det(sI-(A-BK)) = 0.** Fig. 10 shows the response of the cannon angular position with a reference of 90 degrees.

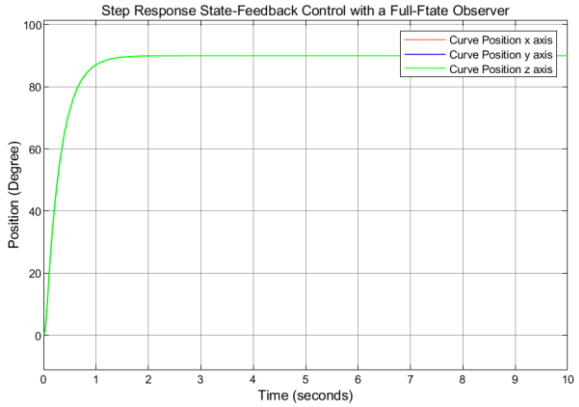

Figure 10. Cannon Simulation Response

The response of the cannon angular position shows that the cannon can reach the desired position of 90 degrees within 1.5 seconds. The response of the simulation results shows good performance when implemented. Fig. 11 shows the response of the control signal given by the controller to the cannon system.

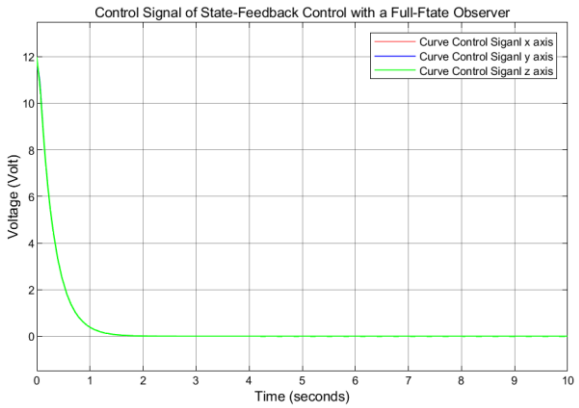

Figure 11. Control Signal Response

The control signal response shows that the voltage provided by the controller to the DC motor is a maximum of 11.7 volts. This voltage does not exceed the input voltage value given by the motor driver to the DC motor, which is 12 volts.

Then, the system was tested to get the same response curve as in the simulation. The method to see the data from the gyroscope on the cannon is to start moving the actuator until the system has a steady state.

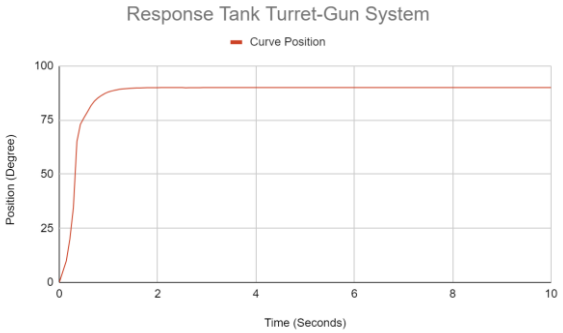

Figure 12. Cannon Implementation Response

The angular position response of the cannon's x-axis, y-axis and z-axis shows that it can reach the desired position of 90 degrees in 0.51 seconds which is the rise time and settling time and 0% overshoot, which is better than the simulation results. In this section, state-feedback control with a full-state observer test has been implemented.

V. CONCLUSIONS

It has been successfully developed to use state-feedback control with a full-state observer for cannon systems, and a pole placement was used to calculate the feedback gain K. The pole placement control approach has also been used to determine the gain of the full-state observer L. The cannon system has a settling time and rise time of 0.51 seconds, and the system is still stable. The system reaction has 0% overshoot, according to the implementation results.

ACKNOWLEDGMENT

The authors would like to thanks Universitas Multimedia Nusantara for supporting this research.

REFERENCES

[1] Putra, D. F. A., & Muharom, A. S. (2021). The stability of cannon position on tank prototype using PID controller. Indonesian Journal of Electrical Engineering and Computer Science, 23(3), 1565-1575.

[2] Tvarozek, J., & Gullerova, M. (2012). Increasing firing accuracy of 2A46 tank cannon built-in T-72 MBT. American International Journal of Contemporary Research, 2(9), 140-156.

[3] Ma, Y., Yang, G., Sun, Q., Wang, X., & Sun, Q. (2021). Adaptive robust control for tank stability: a constraint-following approach. Proceedings of the Institution of Mechanical Engineers, Part I: Journal of Systems and Control Engineering, 235(1), 3-14.

[4] Dursun, T., Büyükcivelek, F., & Utlu, Ç. (2017). A review on the gun barrel vibrations and control for a main battle tank. Defence technology, 13(5), 353-359.

[5] Siradjuddin, I., Amalia, Z., Rohadi, E., Setiawan, B., Setiawan, A., Putri, R. I., & Yudaningtyas, E. (2018). State-feedback control with a full-state estimator for a cart-inverted pendulum

system. International Journal of Engineering & Technology, 7(4.44), 203-209.

[6] Lunze, J., & Lehmann, D. (2010). A state-feedback approach to event-based control. Automatica, 46(1), 211-215.

[7] Esmailzadeh, E., & Taghirad, H. D. (1998). Active vehicle suspensions with optimal state-feedback control. International Journal of Modelling and Simulation, 18(3), 228-238.

[8] Somwanshi, D., Bundele, M., Kumar, G., & Parashar, G. (2019). Comparison of fuzzy-PID and PID controller for speed control of DC motor using LabVIEW. Procedia Computer Science, 152, 252-260.

[9] Pinto, V. H., Gonçalves, J., & Costa, P. (2021). Model of a DC motor with worm gearbox. In CONTROLO 2020: Proceedings of the 14th APCA International Conference on Automatic Control and Soft Computing, July 1-3, 2020, Bragança, Portugal (pp. 638-647). Springer International Publishing.

[10] Aoki, M. (2013). State space modeling of time series. Springer Science & Business Media.

[11] Zadeh, L., & Desoer, C. (2008). Linear system theory: the state space approach. Courier Dover Publications.

[12] Karcanias, N., & Vafiadis, D. (2002). Canonical forms for state space descriptions. Control Systems, Robotics and Automation, 5, 361-380.

[13] Lunze, J., & Lehmann, D. (2010). A state-feedback approach to event-based control. Automatica, 46(1), 211-215.

[14] Ram, Y. M., Singh, A., & Mottershead, J. E. (2009). State feedback control with time delay. Mechanical Systems and Signal Processing, 23(6), 1940-1945.

[15] Bemporad, A., Morari, M., Dua, V., & Pistikopoulos, E. N. (2002). The explicit linear quadratic regulator for constrained systems. Automatica, 38(1), 3-20.

[16] Ruderman, M., Krettek, J., Hoffmann, F., & Bertram, T. (2008). Optimal state space control of DC motor. IFAC Proceedings Volumes, 41(2), 5796-5801.

[17] Panomrattanarug, B., Higuchi, K., & Mora-Camino, F. (2013, September). Attitude control of a quadrotor aircraft using LQR state feedback controller with full order state observer. In The SICE Annual Conference 2013 (pp. 2041-2046). IEEE.

ISSN 2355-3286

Comparison of FIR and IIR Filters for Audio Signal Noise Reduction

Sancho Harmalita Liu[1], Nabila Husna Shabrina[2], Hardson[3]
[1,3] Electrical Engineering, Universitas Multimedia Nusantara, Tangerang, Indonesia
[2] Computer Engineering, Universitas Multimedia Nusantara, Tangerang, Indonesia
[1]sancho.liu@student.umn.ac.id, [2]nabila.husna@umn.ac.id, [3]hardson@student.umn.ac.id

Accepted on 14 June 2023
Approved on 30 June 2023

***Abstract*— An audio signal is often used as a medium for spreading information. However, this signal is easily disrupted by noise from the environment around which the signal is taken, so a filter is needed to eliminate it. In this article, sound signals will be filtered using two types of filters, namely FIR with Hamming window method and IIR with the Butterworth method. Both filters are applied as low pass types with a cut-off frequency of 4000 Hz and an order of 100. Both filters will be employed to filter a 5000 Hz generated audio noise. The SNR and execution time of the filtered signal will then be compared to determine which filter is more effective. The result shows that FIR filters perform better than IIR filters for filtering audio noise.**

***Index Terms*— Digital Filter; Finite Impulse Response- Hamming Window Method; Infinite Impulse Response- Butterworth Method.**

I. INTRODUCTION

In this era, information can be quickly disseminated, and everyone can easily access information through radio, television news broadcasts, and the Internet. Most of this information consists of a one-dimensional audio signal. Therefore, the clarity of the audio signal plays an essential role in transmitting information. Sound signals can experience disturbances in the form of noise. This noise originates from the environment where the sound signal is captured using a microphone. Noise disturbance from the environment is sometimes difficult to predict because there are various types of noise, such as motor vehicles with large cylinder volumes passing by, which cause low-frequency noise; the sound of aircraft jet engines which cause high-frequency noise; or even thunder. Not only found in audio signals, noise can be found in ECG (Electrocardiogram) signals from heart's electrical activity [1], EMG (Electromyography) from muscle's electrical activity [2], and EEG (Electroencephalography) from brain wave [3] [4]. Although information can sometimes be received, it will disrupt the receiver. That is why a filter is needed to reduce the existing noise.

A filter is a device or process that can eliminate unwanted parts of a signal from the input signal and enhance the signals [2]. A filter will only pass through or retain the desired signals [5][6]. There are various filters, such as low pass, high pass, band pass, and others. Previous comparative studies used FIR and IIR filters on ECG, EEG, EMG, and sinusoidal signals. Based on these studies, the FIR filter shows good performance when the filters are implemented to filter noise in ECG, EEG, and EMG signals due to their flexibility, faster execution time, more stable response, and lower phase distortion [1][2][3][4]. Furthermore, the IIR filter is used on sinusoidal and ECG signals because it can use lower orders for similar results and lower computational power and memory usage [7][8][9]. So in this study, FIR and IIR filters with the exact specifications will be applied to filter the audio signal.

FIR was selected due to its easiness in implementation, while IIR was chosen because it requires less memory and processing time when implemented in software [10][11]. The FIR filters and IIR will be implemented to filter audio signal data which added noise at a frequency of 5000 Hz. The noise frequency was chosen to mimic the frequency of electrical interference [12]. This research will compare the effectiveness and performance of both filters based on Signal-to-Noise Ratio (SNR) and the execution time.

II. DIGITAL FILTER

A. Audio Signals

Audio is a wave that is formed when an object vibrates. The contents of this wave consist of a combination of various frequencies, amplitude, and phase. For example, sound can be produced when a drum is struck, causing it to vibrate, and the vibrations propagate through a medium such as air. A signal is a function of one or more variables which can also be defined as changes that can be observed in an entity that can be measured [13]. Therefore, the audio signal is an electronic representation of sound waves that can be directly observed and processed. Humans can hear a sound with frequencies ranging from 20 Hz to 20,000 Hz [14].

B. Digital Filters

A digital filter is a mathematical algorithm that operates on discrete-time signals and samples, allowing it to enhance or reduce aspects of specific signals. Digital filters are more stable and relatively straightforward yet compact than analog filters [6]. These filters are widely used in signal processing and differ from analog filters, which are electronic circuits consisting of resistors, inductors, capacitors, and other components that work with continuous signals [15]. Digital filters contain analog-to-digital converters (ADC) and digital-to-analog converters (DAC) so that digital filters can have input and output as analog signals. Moreover, digital filters are commonly used in digital signal processing, control systems, and communications [16][17][18]. Digital filters can be implemented as Finite Impulse Response (FIR) filters or Infinite Impulse Response (IIR) filters [3]. The difference between FIR and IIR is presented in Table 1.

TABLE I. THE DIFFERENCE BETWEEN FIR AND IIR [10]

FIR Filters	IIR Filters
No phase distortion is introduced into the signal by the filter	Has a non-linear phase response
When realized non-recursively, filter results are always stable	Filter results are not guaranteed to be stable
The effect of using a certain number of bits on applying a filter, such as roundoff noise and coefficient quantization errors, are much more severe	The effect of using a certain number of bits on applying a filter, such as a roundoff noise and coefficient quantization errors, are negligible
Requires more coefficients for sharp cutoff filters	Requires less coefficient for sharp cutoff filter
Easier to synthesize filters with arbitrary frequency responses	Easier to convert analog filters to digital IIR filters

FIR is a filter in which impulse response has a finite duration, meaning it becomes zero within a finite time. This filter several Window methods, such with its characteristics, namely Rectangular, Hanning, Hamming, Blackman, and Kaiser. The Hamming method is the most used Window method, which provides the best results compared to other FIR types for the exact specifications [19]. The coefficient calculation for designing the FIR filter is given in Eqs. (1) [5].

$$h_D(n) = \frac{1}{2\pi} \setminus \int_{-\pi}^{\pi} H_D(\omega) e^{j\omega n} d\omega \quad (1)$$

where $h_D(n)$ represents the ideal impulse response with the equation is presented in Eqs (2).

$$2fc = \frac{\sin(n\omega_c)}{n\omega_c} \quad (2)$$

IIR filters are unique because they use a feedback mechanism, which requires current and previous output data. Although more challenging to design, the IIR filter is more efficient and cheaper. Furthermore, the IIR filter has feedback, so it has an infinite time limit on its impulse response [20]. IIR filters have several methods with distinct characteristics, including Butterworth, Chebyshev, and Elliptic. Based on previous research, the Butterworth method is relatively better than the Chebyshev method if a flat band response is required [21].

The coefficients for designing the IIR low pass filter use the transfer function equation given in Eqs. (3) – (5) [5].

$$H_{LP}(z) = \frac{b_0(z+1)}{z-a} \quad (3)$$

With:

$$a \approx \begin{cases} 1 - 2\pi\left(\frac{F_c}{F_s}\right) & F_c < \left(\frac{F_s}{4}\right) \\ \pi - 1 - 2\pi\left(\frac{F_c}{F_s}\right) & F_c > \left(\frac{F_s}{4}\right) \end{cases} \quad (4)$$

$$b_0 = \frac{1-a}{2} \quad (5)$$

C. Signal-to-Noise Ratio

Noise can be defined as an unwanted signal that interferes with the communication or measurement of other signals [22]. The effect of this noise on the audio signal is that it can change the information carried by the audio signal to the receiver so that the received information differs from what was previously desired [23]. This noise can come from the environment where the sound signal is picked up and cannot be predicted.

Signal-to-Noise ratio is a parameter that compares the desired signal level to the background noise level [14]. SNR is the signal strength ratio to noise strength measured in decibels (dB). A ratio greater than 0 dB or higher than 1:1 indicates there is more signal than noise. Therefore, a higher SNR value will give a better-quality signal. SNR can be calculated by using Eqs. (6).

$$SNR = 10 \log \frac{P_{signal}}{P_{noise}} \quad (6)$$

III. METHODS

The proposed method is presented in Fig. 1. A 5000 Hz noise was added to the audio signal and plotted in the time and frequency domain to see the characteristics of the audio signal. The filtering step will be performed on those signals to remove the noise. A low-pass filter is implemented to pass signals at frequencies below the cut-off value. Because the noise is at a frequency of 5000 Hz, a 4000 Hz cut-off frequency is used. Two types of digital filters are used for comparison: the Finite Impulse Response (FIR) filter with the Hamming Window method and the Infinite Impulse Response (IIR) filter with the Butterworth method. Both types of filters will use the

same sampling frequency, filter order, and cut-off frequency to find out which type of filter performs better. The comparison uses the signal-to-noise ratio (SNR) and the time needed to process the signal.

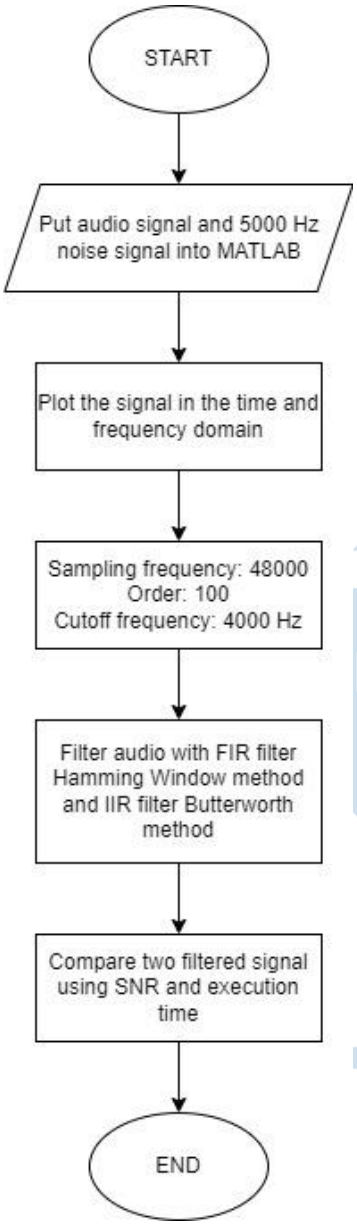

Figure 1. Research method flowchart

IV. Results and Analysis

The audio signal used in this study is obtained from Red Robbo's Workshop [24]. The audio signal was then given a noise at a frequency of 5000 Hz obtained from Sonic Electronix [25]. The sound signal contaminated with the noise is plotted and find the peak of the noise signal.

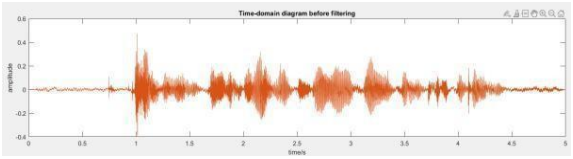

Figure 2. Time Domain Graph of Sound Signal With Noise Before Filtering

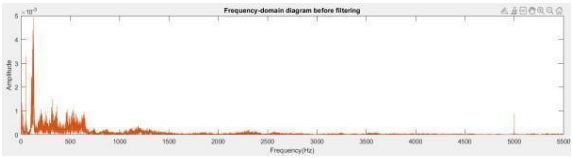

Figure 3. Frequency Domain Graph of Sound Signal With Noise Before Filtering

The time and frequency domain of the unfiltered signal is presented in Figure 2 and Figure 3, respectively. The noise in the signal is located at a frequency of 5000 Hz. For this reason, a cut-off of 4000 Hz is employed with a low pass filter so that frequencies lower than the cut-off will be passed on. The specification of the implemented FIR and IIR filter is shown in Table 2. Two types of filters are used in the form of FIR Hamming Window and IIR Butterworth filters, each with the exact specifications as in Table 2. The filter order is selected based on the trials carried out in the pre-study to get the optimal precise audio signal results on both filters.

TABLE II. The Specification FIR Hamming And IIR Butterworth

Specs	FIR Hamming	IIR Butterworth
Sampling Frequency (Hz)	48.000	48.000
Order	100	100
Cut-off Frequency (Hz)	4000	4000

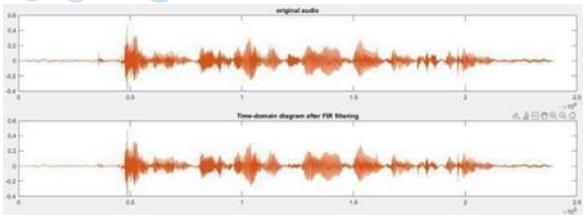

Figure 4. Comparison of time domain noisy audio signals before (top) and after (bottom) filtering using FIR filters

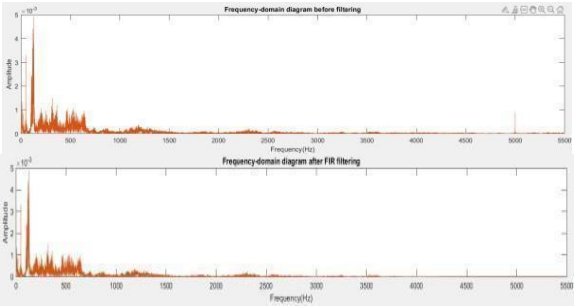

Figure 5. Comparison of frequency domain noisy audio signals before (top) and after (bottom) filtering using FIR filters

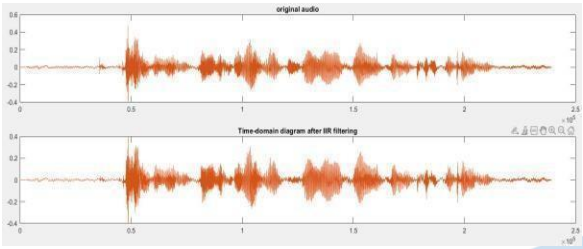

Figure 6. Comparison of time domain audio noisy signals before (top) and after (bottom) filtering using the IIR filter

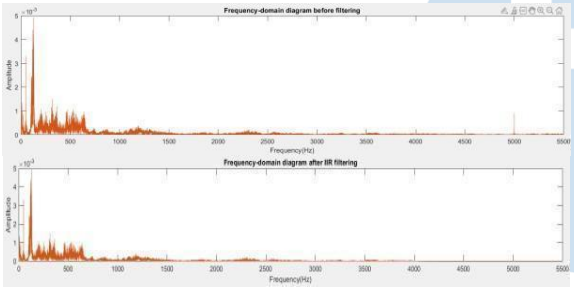

Figure 7. Comparison of frequency domain audio noisy signals before (top) and after (bottom) filtering using the IIR filter

The time domain signal presented in Figure 4 and Figure 6 shows that noise in the signal filtered using both FIR and IIR has decreased. It can be seen that the thickness of the graph generated in the time domain before being filtered is thicker than that of the time domain that has been filtered. This difference in the thickness of the graphs proves the loss of 5000 Hz noise from the signal.

The result in the frequency domain, as seen in Figures 5 and 7, shows a missing signal around the frequency of 5000 Hz. This result shows that both Hamming Window and IIR Butterworth FIR filters can remove noise at a cut-off frequency of 4000 Hz. This result proves that FIR and IIR can eliminate noise at the desired frequency, but the graphs produced by the two filters do not show significant differences. The difference between these filters can be seen in the SNR and execution time. The compassion of the SNR and the execution time of both filters is given in Table 3.

TABLE III. COMPARISON OF EXECUTION TIME AND SNR OF IIR FILTER WITH FIR FILTER

	Without Filter	IIR	FIR
Elapsed Time (s)	–	0,817776	0,213473
SNR (dB)	28.4766	31,4774	31,4782

TABLE IV. EXECUTION TIME FORM MULTIPLE EXECUTIONS

Execution	IIR	FIR
1	0.784473	0.16293
2	0.79077	0.168706
3	0.78685	0.165422
4	0.804127	0.161626
5	0.789127	0.152496
6	0.854054	0.160514
7	0.857525	0.161091
8	0.845725	0.169508
9	0.884793	0.169061
10	0.778916	0.156219
11	0.846445	0.168094
12	0.843364	0.171907
13	0.845329	0.161352
14	0.848843	0.183132
15	0.835147	0.174549
Average	0.8263658667	0.1657738

As seen in Table 3, the time required by the FIR filter is less than that required by the IIR filter, with the value of 0,165773 seconds and 0,826365 seconds, respectively. The execution time in Table 3 is the average result of 15 execution trials, with each execution time result given in Table 4. The time difference is insignificant because both filters require a short processing time. The SNR of the signal filtered using the FIR filter is 31.4782 dB, more significant than the IIR filter, which has an SNR of 31.4774 dB. The results show that the FIR filter with the Hamming Window method is more effective than the IIR filter with the Butterworth method in filtering the noise in the audio signal. Although the difference in execution time and SNR is minimal, implementing both filters in a more extended audio signal will give a more diverse result.

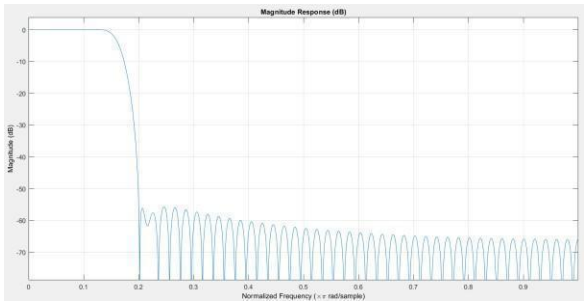

Figure 8. Magnitude response of FIR Hamming Window filter

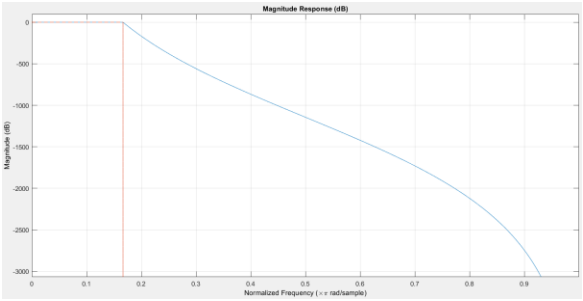

Figure 9. Magnitude response of IIR Butterworth filter

The magnitude response of both the FIR and IIR filter are presented in Figure 8 and Figure 9, respectively. In Figure 8, it can be seen that the cut-off frequency of the audio signal is immediately attenuated. In contrast, the signal is already attenuated in Figure 9 from before the cut-off frequency. In Figure 8, the magnitude response of FIR filter results has more ripples than the results of the IIR filter in Figure 9. However, the FIR filter has a shorter transition band than the IIR filter's transition band. Nevertheless, both filters can filter the noise efficiently.

V. CONCLUSIONS

This study compares the performance of the FIR Hamming method, and IIR Butterworth implemented in a low-pass filter for noise reduction in the audio signal. The result shows that both filters can filter noise effectively and produce clear audio signals. However, the FIR filter with the Hamming Window method is more recommended to be used in filtering 5000 Hz noise in the sound signal because the SNR result by the FIR filter with the Hamming Window is higher than the SNR of IIR filtered signals. In addition, the FIR filter with Hamming Window method has a shorter execution time of 0,165773 seconds than IIR filters with the Butterworth method, which has an execution time of 0,826365 seconds. This time execution difference will be very influential in filtering audio signals that have a long duration.

ACKNOWLEDGMENT

The author would like to thank Universitas Multimedia Nusantara for supporting this research.

REFERENCES

[1] V. V. Reddy, M. Neelaveni, M. Sandeep, S. K. Ahmad, and P. V. Krishna. (2023, April). "Comparison Of Fir And Iir Filters Using Ecg Signal With Different Sampling Frequencies." *International Research Journal of Modernization in Engineering Technology and Science* [Online]. vol. 5, issue 4, pp. 2576-2581. Available: https://www.doi.org/10.56726/IRJMETS35977

[2] C. Leonard, N. H. Sabrina, P. G. A. Bayuntara, and Y. Ariel. (2020, June). "Analisis Keefektifan Penggunaan Filter FIR dan IIR pada Sinyal Pernapasan EMG di dengan Simulasi MATLAB." *Ultima Computing: Jurnal Sistem Komputer* [Online]. vol. 12, pp. 29-34. Available: https://doi.org/10.31937/sk.v12i1.1618

[3] C. Caroline, N. H. Shabrina, M. R. Ao, N. Laurencya, and Vanessa. Lee (2020). Analisis Aplikasi Filter FIR dan Filter IIR dalam Pra-pemrosesan Sinyal Elektroensefalografi. *Ultima Computing: Jurnal Sistem Komputer* [Online]. vol. 12, issue. 1, pp. 40-48. Available: https://doi.org/https://doi.org/10.31937/sk.v12i1.1621

[4] D. Romolo, E. R. Widasari, and B. H. Prasetio. (2020, September). "Analisis Perbandingan Filter Finite Impulse Response, Infinite Impulse Response, dan Discrete Wavelet Transform Pada Kondisi Kelelahan Mental berbasis Sinyal Electroenchephalography." *Jurnal Pengembangan Teknologi Informasi dan Ilmu Komputer* [Online]. vol. 6, issue. 9, pp. 4580-4585. Available: https://jptiik.multi.web.id/index.php/j-ptiik/article/view/11627

[5] A. R. AR and W . Andriani. (2019). "Filtering Sinyal Menggunakan Band Pass Filter". *InfoTekJar: Jurnal Nasional Informatika dan Teknologi Jaringan* [Online]. vol. 4, issue 1, pp. 57-60. Available: https://doi.org/10.30743/infotekjar.v4i1.1194

[6] R. F. Adiati, A. Kusumawardhani, and H. Setijono. (2017). "Analisis Parameter Signal To Noise Ratio dan Bit Error Rate dalam Backbone Komunikasi Fiber Optik Segmen Lamongan-Kebalen". *Jurnal Teknik ITS* [Online]. vol. 6, issue. 2. Available: https://ejurnal.its.ac.id/index.php/teknik/article/view/26079/4673

[7] S. Rani, A. Kaur, and J. S. Ubhi. (2011). "Comparative Study of FIR and IIR Filters for the Removal of Baseline Noises from ECG Signal." *International Journal of computer Science and Information Technologies* [Online]. vol. 2, issue. 3, pp. 1105-1108. Available: https://https://ijcsit.com/docs/Volume%202/vol2issue3/ijcsit2011020332.pdf

[8] N. R. Pai, Chaithra S, Rekha J, and S. R. Bangari. (2019, May). "A Comparative Study of Digital FIR and IIR Band-Pass Filter." *International Research Journal of Engineering and Technology* [Online]. vol. 6, issue. 5, pp. 4244-4247. Available: https://https://www.irjet.net/archives/V6/i5/IRJET-V6I5465.pdf

[9] G. Sreedevi and B. Anuradha. (2016, August). "" *International Journal of Electronics and Communication Engineering and Technology* [Online]. vol. 7, issue. 4, pp 91-99. Available: https://iaeme.com/MasterAdmin/Journal_uploads/IJECET/VOLUME_7_ISSUE_4/IJECET_07_04_011.pdf

[10] S. Zahoor and S. Naseem. (2017, August). "Design and Implementation of An Efficient FIR Digital Filter." *Cogent Engineering* [Online]. vol. 4, issue. 1. Available: https://doi.org/10.1080/23311916.2017.1323373

[11] R. Oshana. (2006). "4 – Overviuw of Digital Signal Processing Algorithms." *Newness* [Online]. Available: https://www.sciencedirect.com/science/article/abs/pii/B9780750677592500065

[12] N. Kularatna, A. S. Ross, J. Fernando, and S. James. (2019), "Design of Background to Surge Protection," in *Transient Protection Systems* [Online]. Elsevier Inc. Available: https://doi.org/10.1016/C2016-0-00423-0

[13] P. Chakravorty, "What Is a Signal? [Online]", September 2018. IEEE Signal Processing Magazine. Available: https://signalprocessingsociety.org/publications-resources/ieee-signal-processing-magazine/what-signal

[14] Y. Syarif. (2018, February). "Rancangan Power Amplifier Untuk Alat Pengukur Transmission Loss Material Akustik Dengan Metode Impedance Tube." *JESCE: Journal Of Electrical and System Control Engineering* [Online]. vol. 1, issue. 2, pp. 55-59. Available: https://doi.org/10.31289/jesce.v1i2.1909

[15] H. Hartono, V. C. Mawardi, and J. Hendryli. (2021). "Perancangan Sistem Pencarian Lagu Indonesia Menggunakan Query By Humming Berbasis Long Short-Term Memory." *JIKSI: Jurnal Ilmu Komputer dan Sistem Informasi* [Online]. vol. 9, issue. 1, pp. 106-111. Available: https://doi.org/10.24912/jiksi.v9i1.11567

[16] E. B. Asmae, K. Loubna, B. Bachir, and Z. Izeddine. (2020, August). Meta-heuristic techniques for optimal design of

analog and digital filter. *Indonesian Journal of Electrical Engineering and Computer Science* [Online]. vol. 19, issue. 2, pp. 669-679. Available: http://doi.org/10.11591/ijeecs.v19.i2.pp669-679

[17] Q. Wang, H. Shibata, A. Liscidini and A. C. Carusone. (2018, March). "A Digital Filtering ADC With Programmable Blocker Cancellation for Wireless Receivers." *IEEE Journal of Solid-State Circuits* [Online]. vol. 53, issue. 3, pp. 681-691. Available: https://doi.org/10.1109/JSSC.2017.2766213

[18] G. Deng, J. Chen, J. Zhang, and C. -H. Chang (2019). "Area- and Power-Efficient Nearly-Linear Phase Response IIR Filter by Iterative Convex Optimization." *IEEE Access* [Online]. vol. 7, pp. 22952-22965. Available: https://doi.org/10.1109/ACCESS.2019.2899107

[19] A. Bustamin and A.A Paryogi. (2019). "Perbandingan Kinerja Filter Butterworth Berdasarkan Spesifikasi Frekuensi untuk Pengolahan Sinyal Suara." *Jurnal Teknologi Informasi Techno.Com* [Online]. vol. 18, issue. 4. Available: https://doi.org/10.33633/tc.v18i4.2714

[20] M. S. R. Islamiyah, R. Saptono, and H. Hadiwiyatno. (2021, March). "Implementasi Metode Transformasi Biliniear Pada Filter Digital Infinite Impulse Response (IIR) Menggunakan Raspberry Pi." *Jurnal Jaringan Telekomunikasi* [Online]. vol. 11, issue. 1. Available: https://doi.org/10.33795/jartel.v11i1.28

[21] S. Bakshi et al., "Designand Comparison Between IIR Butterwoth and Chebyshev Digital Filters Using Matlab," in *2019 International Conference on Computing, Communication, and Intelligent Systems (ICCCIS)*, Greater Noida, India, 2019, pp. 439-446. [Online]. Available: https://doi.org/10.1109/ICCCIS48478.2019.8974554

[22] G. C. Setyawan and M. P. Nawansari. (2022, September). "Kinerja Penapisan Gaussian dan Median Dalam Pelembutan Citra." *Journal of Information Technology* [Online]. vol. 2, issue. 2, pp. 1-4. Available: https://doi.org/10.46229/jifotech.v2i2.433

[23] M. Iqbal, H. Walidainy, and E. Elizar. (2019). "Analisis Filter Kalman untuk Menghapus Noise pada Sinyal Suara." *Seminar Nasional dan Expo Teknik Elektro 2019*. Available: http://snete.usk.ac.id/2019/wp-content/uploads/2019/12/Naskah-1-Muhammad-Iqbal.pdf

[24] Red Robbo's Workshop. (2018, July 8). *Speech Audio Quality Test*. Accessed: 2022. [Online Video]. Available: https://www.youtube.com/watch?v=o8dEgTMZ81g

[25] Sonic Electronix. (2016, January 1). *5000 Hz Test Tone*. Accessed: 2022. [Online Video]. Available: https://www.youtube.com/watch?v=cx1VQISKvhc.

ISSN 2355-3286

Soil Moisture Control System for Lettuce Seeds: Time-based Alternative Approach

Fakhruddin Mangkusasmito[1], Ageng Rilla Aldonanda[2], Dista Yoel Tadeus[3]
[1,3]STr. Teknik Listrik Industri, Sekolah Vokasi Universitas Diponegoro, Semarang, Indonesia
[2] STr. Teknologi Rekayasa Otomasi, Sekolah Vokasi Universitas Diponegoro, Semarang, Indonesia
[1]fakhm17@lecturer.undip.ac.id, [3]distayoel@gmail.com

Accepted on 16 June 2023
Approved on 30 June 2023

***Abstract*— The utilization of lettuce leaves as a nutritious dish has made its demand relatively high. This research presents a moisture control method to optimize seed growth for lettuce. The prototype system has been developed using Arduino Mega, DF Robot soil moisture humidity sensor, and DC spraying pump for testing three different control scenarios, the open loop control system (time-based), the Proportional control system, and the combination of open loop and Proportional control method as an alternative. The results show that each control method can achieved the desired moisture of rockwool at 60%. Also the combination of open loop and Proportional control can lessen energy usage of the system up to 51% compared to common open loop method.**

***Index Terms*— energy efficiency; lettuce; moisture control; open loop; Proportional control.**

I. INTRODUCTION

As one of the most demanded vegetable commodities, lettuce (Lactuca sativa L.) has been cultivated both using conventional and hydroponic methods. The hydroponic method aims to increase productivity, especially in narrow land, research shows that the hydroponic cultivation method for lettuce plants is feasible and still provides financial benefits[1][2]. Temperature and humidity are environmental variables that are very important to consider in cultivating hydroponic lettuce in a greenhouse system. Lettuce growth will be optimal in the air temperature range of 25°C to 28°C and humidity ranging from 60% to 78%. Unstable temperature and humidity conditions may cause the plants to wilt and interfere with the development of seedlings[3][4]. In order for lettuce plants to germinate properly, soil humidity needs to be maintained at a value of 60%[5]. Control of soil moisture is generally done by spraying water as needed, to achieve the desired humidity level[6], [7].

For commercial use, automatic spraying devices are generally time-based (e.g., Spraying Systems co, PulsaJet, AutoJet, AQUALIN, Yardsmith and Universal)[8], the user will be asked to set the desired spraying hours, and in some products, the length of time can also be adjusted according to user needs. Even though there have been many studies that have developed based on closed-loop systems using sensors and microcontroller, such as the DHT 11 sensor,[9]–[11] the open-loop spraying system is still considered efficient and commonly used. On the other hand, in closed-loop control schemes, proportional control systems are also widely used for various industrial applications[12]–[15], this control system was chosen because it is relatively simple and easy to fine-tune[16].

This research will examine the effectiveness of time-based automatic spraying (open-loop control) in terms of maintaining the desired soil or rockwool moisture value, with the addition of a proportional control method (closed-loop) when the spraying schedule is executed. It is hoped that the combination of these control methods can improve the performance of similar spraying systems that are already on the market, especially in term of energy conservation. This system will be built using Arduino Mega microcontroller, DF Robot soil Moisture humidity sensor, real-time clock (RTC), and actuator in the form of a DC spraying pump, and Micro SD Module for data logging purpose.

II. METHODS

A. Block Diagram of Component

The system is developed based on Arduino Mega 2560, to operate the system properly, the main component used for this research is shown in the Figure 1. below.

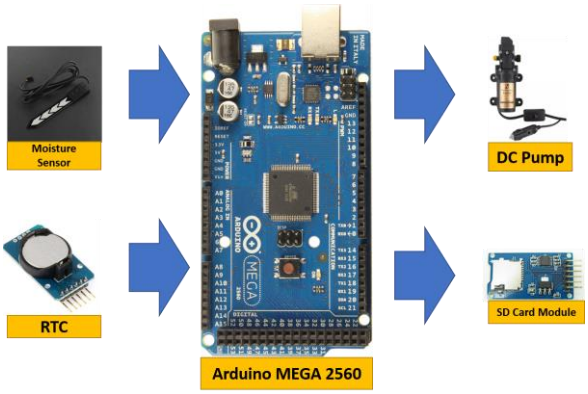

Figure 1. Main Components of System

The main parts of the system shown in Figure 1 are as follow:

1. Arduino Mega 2560 works as a place to process all the data used to drive the mini pump, as well as process data from sensors.
2. Moisture sensors are used to read the humidity in the planting medium for control purposes and logging data.
3. Time RTC is used as a spraying time marker which is then set in the Arduino program which will later be forwarded to the DC pump actuator.
4. The DC pump is used to carry out the process of spraying water from the water storage area to the planting medium through a PVC hose. The use of the pump is assisted by a noozle outlet to produce water in the form of a light mist.

B. *Block Diagram of Control System*

This research use both open loop and closed loop control system for different scenario of experiments. The setpoint is set to 60% of soil humidity. The open-loop control diagram is shown in Figure 2.

Figure 2. Open Loop Control System

In the open loop control method, the operation time must be set before, in order to activate the spraying mechanism to achieve setpoint. RTC is used to give accurate time of operation. Close loop control method is used for continuously regulate the humidity. The closed-loop control diagram is shown in Figure 3.

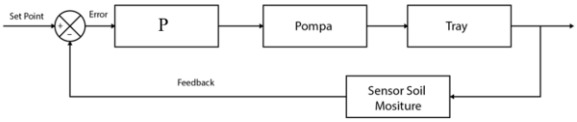

Figure 3. Closed Loop Control System

The closed-loop control system used proportional method, with the gain of proportional (Kp) is obtain through several experiments and performance evaluation. The proportional control system implemented in this study is the time-proportional method, which can be found in industrial temperature controllers such as Autonics products[17], when the control signal output (CO) from proportional control = 100%, the system will be active for 5 seconds, or according to the following equation.

$$T_s = C0.5second \quad (1)$$

with T_s is time of spray.

C. *Hardware Design and System Feature*

The system is build using galvanized iron material, with three segments for seedling cultivation. The three-dimensional design of the soil moisture control system is shown in Figure 4 below.

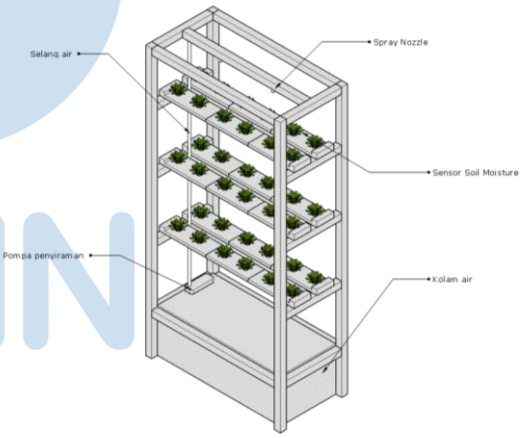

Figure 4. 3D Design of System

The specifications for this soil moisture control system are as follows:

1. The dimensions are 1.8 meters x 1 meter.
2. Using 220 VAC power
3. Using 12VDC power supply
4. Using a 6mm Plastic Nozzle
5. Using the Arduino Mega 2560 Microcontroller
6. Using the waterproof DF Robot Soil Moisture Humidity Sensor
7. Using Real Time Clock is an electronic clock in the form of a chip that can accurately calculate time (from seconds to years) and maintain/store data of that time in real time.

8. Using a MicroSD Module as a data logger storage of spraying record.
9. Using LCD I^2C 20x4 as display
10. Using a 12V 100 PSI SINLEADER Pump.
11. There are 3 modes in 1 sprinkle system:
    - Mode 1: Time Base (Open loop control)
    - Mode 2: Continous control (proportional control)
    - Mode 3: Combination of Time-Base and Proportional control
12. Three-segment for seedling cultivation.

III. Results and Analysis

The experiment was carried out in January-February 2023, in the Undip Vocational School area, the system was placed in a semi-outdoor area which still got sunlight and a little bit of rain during rainy days. The interval of data acquisition is 1 minute.

A. *Open Loop Experiment*

Open loop testing is carried out to see the effect of the actuator on changes in the variable to be controlled, namely soil moisture. The results of this experiment will be used as a reference for choosing the duration of plant spraying. The experiment is conduct at 09.00 WIB, from the initial humidity condition of 30% to reach the desired setpoint value of 60%. The result of experiment is shown in Figure 5.

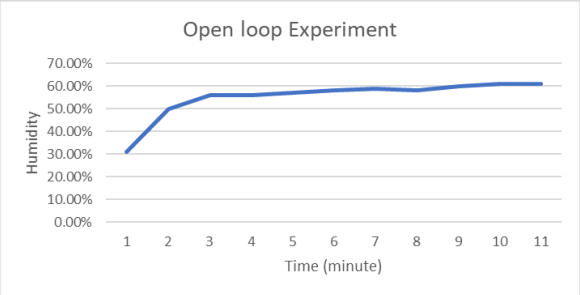

Figure 5. Open Loop Test Results

Based on the Figure 5, the actuator can achieve the desired setpoint within 10 minutes, therefore we based the spraying duration for open loop control in accordance with the result.

B. *Mode 1: Time Base (Open Loop Control)*

Open loop testing is carried out to see the effect of the actuator on changes in the variable to be controlled, namely soil moisture. The results of this experiment will be used as a reference for choosing the duration of plant spraying. The experiment is conduct at 09.00 WIB, from the initial humidity condition of 30% to reach the desired setpoint value of 60%. The result of experiment is shown in Figure 5.

TABLE I. Mode 1: Time Base (Open Loop Control) Test Result

Day	1st Watering (09.00-09.10)		2nd Watering (15.00-15.10)	
	Start Humidity (%)	End Humidity (%)	Start Humidity (%)	End Humidity (%)
1	41	65	48	64
2	51	67	55	68
3	53	73	52	68
4	55	73	59	76
5	51	74	56	68

The test results show that a time-based automatic watering system can bring soil moisture to an ideal value (60% -78%), but if it is expected that the system "only needs" to reach a lower threshold value of 60%, then the system experiences energy wastage and less optimal.

In this test, monitoring was also carried out at other than the time of spraying, at 13.00-14.00 and 17.00-18.00, to monitor the soil humidity outside of spraying schedule. In general, soil moisture is maintained at the ideal plant value, but on certain day, especially during hot weather, humidity can drop less than the recommended ideal value. As on the second day of testing at 13.00-14.00 the soil moisture dropped to a value of 53% as shown in Figure 6 below.

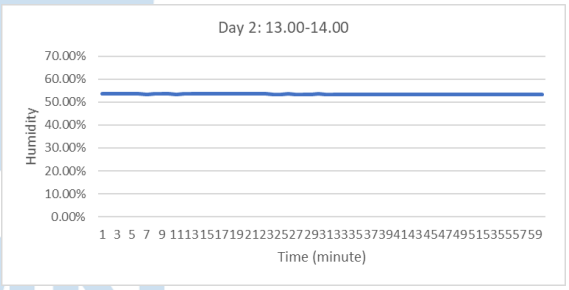

Figure 6. Soil Humidity Day 2 13.00-14.00

C. *Mode 2: Continous Control (Proportional Control)*

In Mode 2, experiments is carried out using several proportional gains (Kp). The test was carried out 5 times with an initial value of humidity = 43% and set point of 60% with duration of 1 hour. The results of the test will be evaluated by selecting the best settling time (ts) and root mean square error (RMSE) values. The results of the test are shown in Table 2 below.

TABLE II. Proportional Control Test Results

Test	Kp	ts (minute)	overshoot (%)	RMSE %)
1	2	20	0	5,80
2	3	18	0	3,80
3	4	13	0	7,11
4	5	6	0	2,48
5	6	4	0	3,64

Based on the result, the proportional control system can achieve the desired humidity of 60% with no overshoot occurred. The Kp value of 5 is choosen,

because it gave the minimum RMS, the transiet response of Kp value = 5 shown in Figure 7.

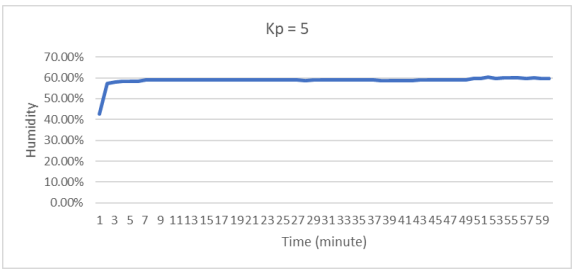

Figure 7. Proportional Test Result with Kp = 5

D. Mode 3: Combination of Time-based and Proportional Control

A closed loop control system that is carried out continuously will be able to regulate soil moisture as desired. However, taking into account the results of the mode 1 test, that the humidity value can be maintained in the ideal range naturally, it is necessary to optimize the time-based method. In this mode, the proportional control system (with Kp=5) will be used simultaneously during the time-based method of spraying, specifically at 09.00-10.00 and 15.00-16.00. This is so that the system does not spray until it exceeds the ideal humidity threshold value = 60%. And the logical consequence is that there will be energy savings because the spray pump is not operating. To measure energy consumption when the system is operating, an energy meter is used. The tool will display the total power used and used as the basis for calculating the total energy consumption of the system. The measurement results from the energy meter when the system is operating is shown in Figure 8 below.

Figure 8. Power Measurement Result

The test show that the power used for operating the system is 44,1 watt.

The experiment of this mode is carried out for 5 days. The result of experiment on day one at 09.00-10.00 is shown in the Figure 9.

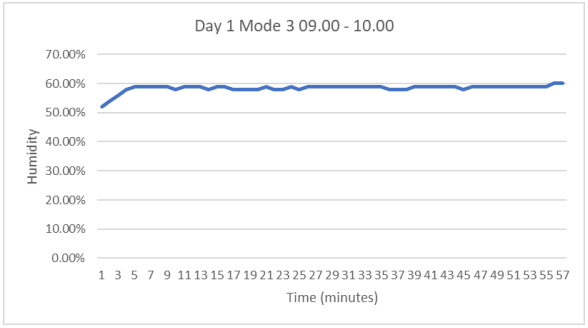

Figure 9. Result of Mode 3 Day 1 at 09.00-10.00

The Figure 9 shown that the system can relatively maintain the soil humidity at 60% during an hour period, and we can see the proportional control took over when the humidity drops too low or going too high (see red dash block). The experimental results obtained in 5 tests showed relatively the same results. The result of experiment on day one at 15.00-16.00 is shown in the Figure 10.

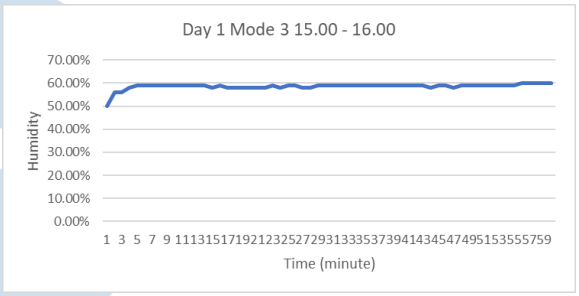

Figure 10. Result of Mode 3 Day 1 at 15.00-16.00

The result of experiment on day two at 09.00-10.00 is shown in the Figure 11.

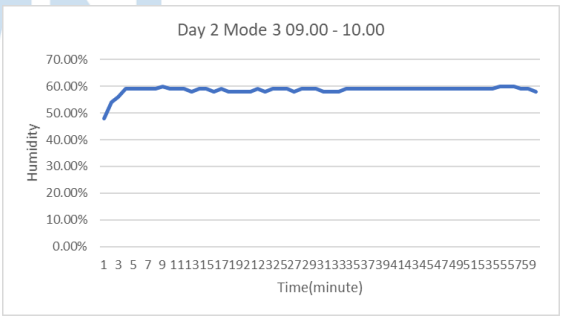

Figure 11. Result of Mode 3 Day 2 at 09.00-10.00

The result of experiment on day two at 15.00-16.00 is shown in the Figure 12.

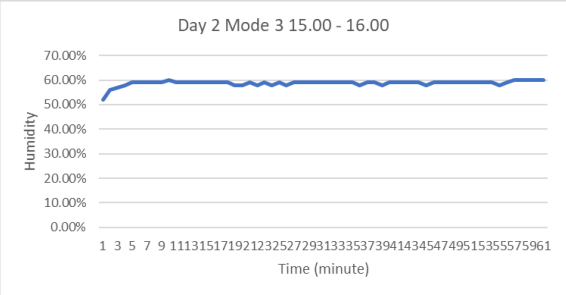

Figure 12. Result of Mode 3 Day 2 at 15.00-16.00

The active duration of the pump is also calculated to measure the total energy consumption when Mode 3 is run for 1 hour, the sample taken is the active time at 09.00-10.00. The calculation of total energy consumption for days 1 - 5 at 09.00-10.00 are shown in Table 3 below.

TABLE III. ENERGY CONSUMPTION OF MODE 3 AT 09.00-10.00

Day	Pump Active Periode (second)	Total Energy (Joule)
1	288	12,700
2	289	12,745
3	289	12,745
4	290	12,789
Average		12,745

The result shows the average energy consumption for Mode 3 is 12,745 joule while using Mode 1 with the duration of 10 minute spraying equal to energy consumption of 26,460 joule.

IV. CONCLUSIONS

The experimental results show that the designed system works well to control soil moisture which is ideal for the growth and development of lettuce seedlings. In particular, Mode 3 presents an alternative to time-based open-loop control that is commonly used, by combining it with a proportional control system, it can be seen that energy use can drop significantly from 26,460 joules to a value of 12,745 joules.

Although it looks promising the use of a time-based control system needs to pay close attention to the geographical location and weather of the farm itself. Closed cultivation methods such as greenhouses will be more effective in reducing environmental influences even though the investment costs may be greater.

REFERENCES

[1] N. Eniza Riani, Karwati Zawani, "RESPON TANAMAN SELADA (Lactuca sativa L.) TERHADAP BERBAGAI KOMPOSISI MEDIA ORGANIK," *Crop Agro*, no. 1, 2018.

[2] R. A. Umikalsum, "Analisis Usahatani Tanaman Selada Hidroponik pada Kebun Eve's Veggies Hydroponics Kota Palembang," *Societa: Jurnal Ilmu-Ilmu Agribisnis*, vol. 8 (1), 2020.

[3] N. Yamori, C. P. Levine, N. S. Mattson, and W. Yamori, "Optimum root zone temperature of photosynthesis and plant growth depends on air temperature in lettuce plants," *Plant Mol Biol*, vol. 110, no. 4–5, 2022, doi: 10.1007/s11103-022-01249-w.

[4] . W. Tibbitts and G. Bottenberg, "Growth of Lettuce Under Controlled Humidity Levels1," *Journal of the American Society for Horticultural Science*, vol. 101, no. 1, 2022, doi: 10.21273/jashs.101.1.70.

[5] I. K. A. Andika, Y. Setiyo, and I. P. G. Budisanjaya, "Analisis Iklim Mikro di dalam Sungkup Plastik pada Budidaya Tanaman Selada Keriting (Lactuca sativa var. cripa L).," *Jurnal BETA (Biosistem dan Teknik Pertanian)*, vol. 7, no. 1, 2018, doi: 10.24843/jbeta.2019.v07.i01.p08.

[6] A. Rio, B. Si. Nugroho, and Hasanuddin, "Rancang Bangun Pengendalian Kelembapan Tanah dan Suhu Lingkungan Tanaman Berbasis NodeMCU ESP8266," *Prisma Fisika*, vol. 10, no. 1, pp. 40–47, 2022, [Online]. Available: https://jurnal.untan.ac.id/index.php/jpfu/article/view/53548

[7] S. K. Risandriya, "Pemantauan dan Pengendalian Kelembapan, Suhu, dan Intensitas Cahaya Tanaman Tomat dengan Logika Fuzzy Berbasis IoT," *Journal of Applied Electrical Engineering*, vol. 3, no. 1, pp. 9–14, Jun. 2019, doi: 10.30871/jaee.v3i1.1394.

[8] R. Berenstein and Y. Edan, "Automatic Adjustable Spraying Device for Site-Specific Agricultural Application," *IEEE Transactions on Automation Science and Engineering*, vol. 15, no. 2, 2018, doi: 10.1109/TASE.2017.2656143.

[9] A. M. Khafi, "Sistem Kendali Suhu Dan Kelembaban Pada Greenhouse Tanaman Sawi Berbasis IoT," *Generation Journal*, vol. 3, no. 2, p. 37, Aug. 2019, doi: 10.29407/gj.v3i2.12973.

[10] Z. Zaida, I. Ardiansah, and M. A. Rizky, "Rancang Bangun Alat Pengendali Suhu dan Kelembaban Relatif pada Rumah Kaca dengan Informasi Berbasis Web," *Jurnal Teknotan*, vol. 11, no. 1, Jul. 2017, doi: 10.24198/jt.vol11n1.2.

[11] I. P. G. Budisanjaya and I. N. Sucipta, "Rancang Bangun Pengendali Suhu, Kelembaban Udara dan Cahaya dalam Greenhouse Berbasis Arduino dan Android," *Jurnal Ilmiah Teknologi Pertanian Agrotechno*, vol. 3, no. 2, p. 325, Feb. 2019, doi: 10.24843/jitpa.2018.v03.i02.p03.

[12] M. R. Brinton, E. Barcikowski, T. Davis, M. Paskett, J. A. George, and G. A. Clark, "Portable Take-Home System Enables Proportional Control and High-Resolution Data Logging With a Multi-Degree-of-Freedom Bionic Arm," *Front Robot AI*, vol. 7, Sep. 2020, doi: 10.3389/frobt.2020.559034.

[13] N. Yang, Y. Li, and L. Shi, "Proportional Tracking Control of Positive Linear Systems," *IEEE Control Syst Lett*, vol. 6, pp. 1670–1675, 2022, doi: 10.1109/LCSYS.2021.3130638.

[14] Q. Tang, C. Wu, J. Wu, C. Qin, L. Jiang, and G. Wang, "Electro-hydraulic Proportional Control System of Hole Distance for Rape Seedling Rotary Tillage Combined Transplanter," *Nongye Jixie Xuebao/Transactions of the Chinese Society for Agricultural Machinery*, vol. 51, no. 10, pp. 61–68, Oct. 2020, doi: 10.6041/j.issn.1000-1298.2020.10.008.

[15] Y. R. Ko and T. H. Kim, "Feedforward plus feedback control of an electro-hydraulic valve system using a proportional control valve," *Actuators*, vol. 9, no. 2, Jun. 2020, doi: 10.3390/ACT9020045.

[16] K. Ogata, *Modern Control Engineering 5th Edition*. 2002. doi: 10.1109/TAC.1972.1100013.

[17] M. Fakhruddin, Y. Yuniarto, P. Ari Bawono, W. Heru, A. Eko, and T. Dista Yoel, "Realization of industrial based temperature heating control module using TK4S-T4RN," *Mater Today Proc*, vol. 63, 2022, doi: 10.1016/j.matpr.2022.04.088.

ISSN 2355-3286

Simple and Accurate Instrumentation Device to Detect Loose-End Defective Cigarettes

Dista Yoel Tadeus[1], Fakhruddin Mangkusasmito[1], Ari Bawono Putranto[2], Muhamad Ramzy Raihan[2]
[1,2] Electrical Engineering, Vocational School, Diponegoro University, Indonesia
[3,4] Automation Engineering, Vocational School, Diponegoro University, Indonesia
[1]distayoel@live.undip.ac.id, [2]fakhm17@lecturer.undip.ac.id, [3]aribawonoputranto@lecturer.undip.ac.id

Accepted on 22 June 2023
Approved on 30 June 2023

***Abstract*— Loose-end defect on the tip of the cigarette is a common problem found on production lines. Large companies use computerized sophisticated machines to detect and reject it automatically. However, the same solution can not be implemented in small or home industries because the investment cost is too high. This paper presents the development of simple electronic instrumentation to detect loose-end defects in cigarettes. It relies on the signal acquisition of a photoelectric transceiver mechanism that is converted and processed digitally to relatively quantify the difference between the good and defect. Motor-driven cigarette rotator device was built specially to test the performance of the instrumentation system. Loose-end defects are made artificially by removing 0.2 gr tobacco from the tip of a normal cigarette. The average quantifying relative value was found above 58.5%, this indicates that the system has good contrast properties. At the speed of 10,000 cigarettes/min, the average accuracy is 90.5%, and at 17,500 cigarettes/min, the average accuracy is 65.3%.**

***Index Terms*— cigarette quality; loose-end defective cigarette; photoelectric device.**

I. INTRODUCTION

The Indonesian cigarette industry has experienced significant growth over the past few decades [1], [2]. One of the factors contributing to this growth is the implementation of machine processes in the production of cigarettes [3]. These machines have revolutionized the way cigarettes are manufactured, providing numerous benefits to both the industry and consumers. However, one persistent issue that continues to plague the industry is the occurrence of loose-end defects [4]. This defect refers to the presence of unfinished or loose tobacco at the end of a cigarette, resulting in a subpar smoking experience for consumers. The loose-end defect can arise due to several reasons during the manufacturing process. Improper cutting of the tobacco, inadequate application of adhesive, or faulty machinery can all contribute to this defect. When a consumer lights a cigarette with a loose-end, they may experience a faster burn rate, uneven draw, and increased tobacco wastage. These issues not only affect the smoking experience but also lead to dissatisfaction among consumers. Smokers expect a consistent and enjoyable smoking experience from the cigarettes they purchase. The loose-end defect directly undermines this expectation. When a cigarette burns too quickly or unevenly, it affects the taste and overall satisfaction of the smoker. Consumers may also feel cheated as they are paying for tobacco that ends up being wasted due to loose-ends.

One way to tackle the loose-end defect is by implementing improved manufacturing techniques. Cigarette manufacturers can invest in state-of-the-art machinery that ensures precise and consistent packing of tobacco and paper. By using advanced automation and quality control measures [5], the likelihood of loose-ends can be significantly reduced. These techniques can help create cigarettes with tightly packed tobacco that stays intact throughout the smoking process. However, the same solution can not be implemented in small or home industries because the investment cost is too high. Loose-end defect detection based on photoelectric devices is a common method used in several patent sources [6]–[12]. A machine vision-based method for detecting the loose-end defect of a cigarette was also employed [13]–[15].

This paper presents the development of simple and low-cost electronic instrumentation to detect loose-end defects in cigarettes. It relies on a photoelectric infrared transmitter and phototransistor receiver. One of the key advantages of this photoelectric device is its simplicity and low cost. The phototransistor receiver is placed at the tip of the device and emits a beam of light. When a cigarette is inserted, the beam is interrupted. The microcontroller analyzes the interruption pattern to determine whether the cigarette has a loose-end defect. Motor-driven cigarette rotator device was built specially to test the performance of the proposed instrumentation system. There are two parameter qualifiers to indicate its performance: contrast properties of the measured signal and the accuracy of detection capability, both are normalized in percentage.

II. METHODS

A. Hardware Block Diagram

The instrumentation system mainly relies on infrared light transmission through the tip of the cigarette and its intensity was received by the photodiode to produce a small equivalent voltage. This voltage was amplified by a signal conditioner to a reasonable value before it was converted to a digital value and calculated by a microcontroller to relatively quantify the value of the good and defective cigarettes. Figure 1 shows the flow of signal on the main hardware of the instrumentation system.

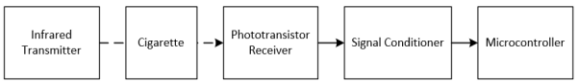

Figure 1. Main Hardware Block Diagram

B. Photoelectric Components Arrangement

Infrared transmitter and phototransistor receiver were placed at certain gaps to ensure physical non-contact with cigarettes so it can move freely between them. Figure 2 shows the arrangement of photoelectric components: infrared transmitter (1), cigarettes (3), and PT334-6B phototransistor receiver (2). It uses three infrared transmitters to improve light intensity reception on the receiver.

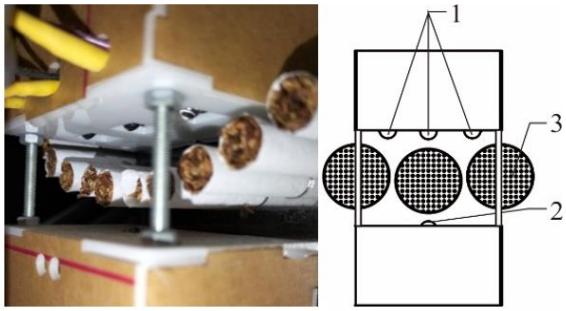

Figure 2. The Arrangement of Photoelectric Components

Figure 3 shows a single infrared transmitter based on High Power LED (HPL) with 3 Watts power consumption and emits a 940 nm wavelength of infrared light. These LED are designed to provide a higher output of infrared radiation compared to standard infrared LED. With advancements in technology, high power infrared LEDs have become more efficient, compact, and capable of emitting light in a narrower wavelength range.

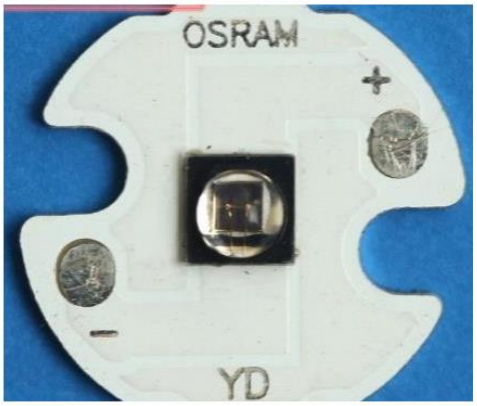

Figure 3. 3 Watts 940nm Infrared HPL

Figure 4 shows a typical 5mm generic phototransistor infrared receiver. Infrared phototransistors offer several advantages over other types of infrared detectors, such as infrared photodiodes. One of the key advantages is their ability to amplify the current, which allows for greater sensitivity and detection range. Another advantage is their response time. Infrared phototransistors can detect and amplify infrared light signals at a faster rate compared to other infrared detectors.

Figure 4. A Typical 5mm Infrared Phototransistor

C. Signal Conditioner Circuit

Figure 5 shows the electronic circuit for a signal conditioner that utilizes an operational amplifier as a non-inverting voltage amplifier with a gain of 3. The non-inverting amplifier is a type of operational amplifier (op-amp) configuration that amplifies an input signal while maintaining the same polarity. It is widely used due to its high input impedance, low output impedance, and excellent gain accuracy. The basic non-inverting amplifier circuit consists of an op-amp, two resistors, and an input and output terminal. The input signal is applied to the non-inverting terminal of the op-amp, while the inverting terminal is connected to ground. The output signal is taken from the junction between the resistor connected to the inverting terminal and the op-amp's output.

The non-inverting amplifier operates based on the principle of negative feedback. When an input signal is applied to the non-inverting terminal, the op-amp

amplifies it and produces an output signal. This output signal is fed back to the inverting terminal through the resistor connected between the output and inverting terminal.

The feedback loop creates a voltage divider between the input and output resistors, which determines the gain of the amplifier. The gain of the non-inverting amplifier is given by the formula:

$$Gain(A) = 1 + \frac{R_F}{R_{in}} \quad (1)$$

where R_F is the feedback resistor and R_{in} is the input resistor. The gain is always greater than 1, making the non-inverting amplifier an amplification device. The output voltage is connected to the Analog to Digital Converter (ADC) pin of a microcontroller. The analog voltage is then converted to an equivalent digital value to indicate infrared light intensity received by the phototransistor. The ADC is a 10-bit successive approximation type. It has a resolution of 1024, which means it can divide the input voltage range into 1024 discrete steps. The ADC operates based on the principle of comparing the input voltage with a known reference voltage. It generates a digital value proportional to the input voltage within the 0-1023 range.

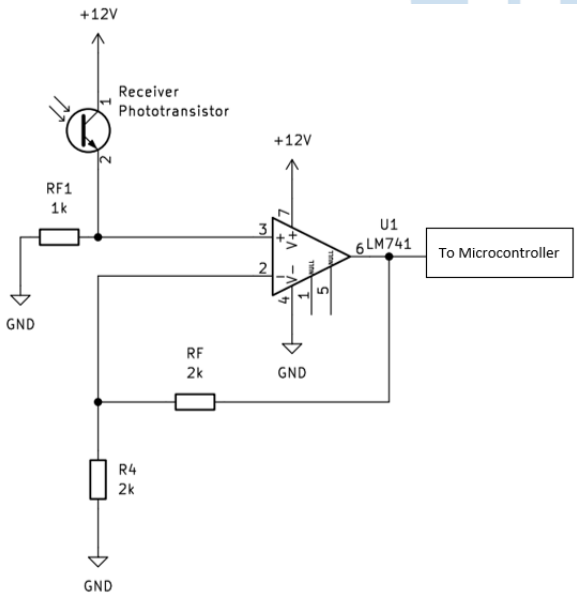

Figure 5. Non-inverting Amplifier Circuit Diagram

D. Mechanical Motor Driven Cigarette Rotator

A mechanical rotator device was specially built to test the performance of the instrumentation system. It can mount up to 50 cigarettes. The rotator is motor driven and its speed can be adjusted by a dedicated controller up to 17,500 cigarettes/min. Figure 6 shows the isometric view of the rotator and Figure 7 shows its side view, showing its motor and encoder. The mechanical rotator has built from five main parts: skid and frame (1), rotator wheel (2), human-machine interface (3), DC motor and speed controller (4), and encoder (5). Figure 8 shows the actual build of the mechanical rotator showing its cigarette wheel holder.

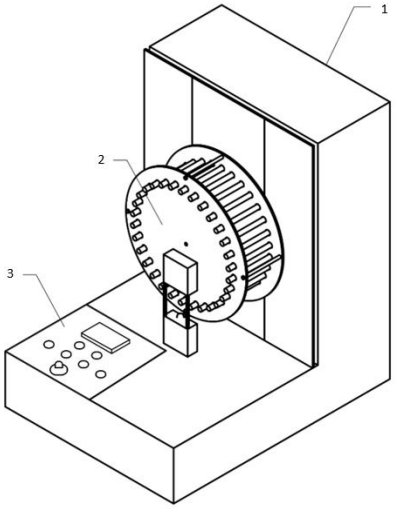

Figure 6. 3D Isometric View of Mechanical Cigarette Rotator

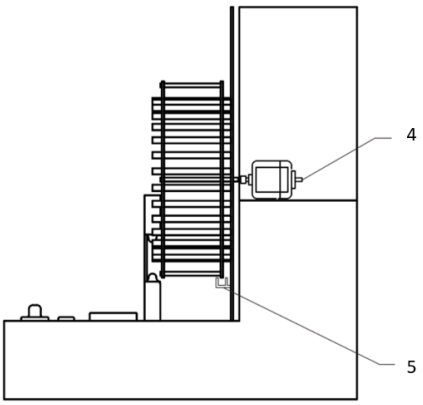

Figure 7. Side View of Mechanical Cigarette Rotator

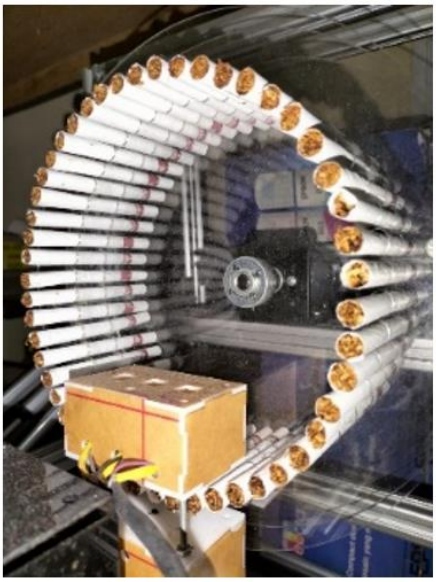

Figure 8. Actual Cigarette Rotator With Capacity of 50 Cigarettes

III. Results and Discussion

The experiment was conducted to obtain two performance parameters of an instrumentation system that has been tested on simulated environment conditions using a mechanical rotator:

- Contrast properties of the measured signal

This parameter indicates a relative range of light intensity that is able to be received by the instrumentation system. A larger value is good, it means the system has a reasonable range to easily distinguish a normal cigarette from a defective cigarette.

- Accuracy of detection

This parameter indicates the system's ability to detect defective cigarettes. The test was conducted in two configurations: altering rotator speed and altering the amount of artificially loose-end defective cigarettes which are placed randomly on the rotator wheel.

The artificial loose-end defective cigarettes were made by removing 0.2 gr tobacco from the tip of a single normal cigarette as shown in Figure 9.

Figure 9. Normal and Artificially Loose-End Defective Cigarette

Figure 10 shows a series of digital values obtained from the calibration batch using a 40/50 configuration (40 normal cigarettes, 10 loose-end defective cigarettes, and 50 total cigarettes). This data is used to define a loose-end range of digital value and a range of normal cigarette's digital value. The relative difference between them is defined as the contrast properties of the measured signal and calculated using Equation 2.

Figure 11 shows the example of collected data from test batch 40/50 at a speed of 10,000 cigarettes/min, where the actual speed employed at the production level was around 8000 cigarettes/min. Figure 12 shows the data at a speed of 17,500 cigarettes/min. Actually, there are digital values greater than the upper limit of defined loose-end digital value. They were produced by light transmission through the gap between adjacent cigarettes on the mechanical rotator, as shown in Figure 13. Those values are excluded from the calculation.

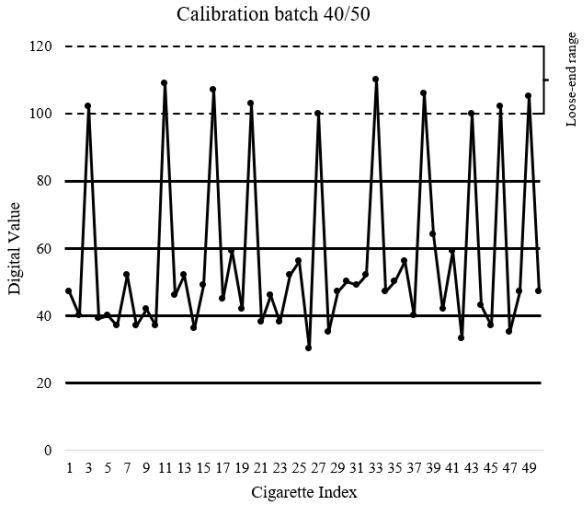

Figure 10. A Series of Digital Values Obtained From Calibration Batch

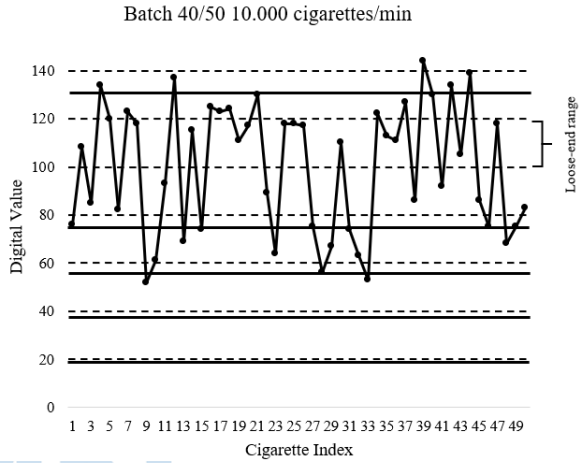

Figure 11. Example of Digital Value Obtained From Batch 40/50 10,000 cigarettes/min

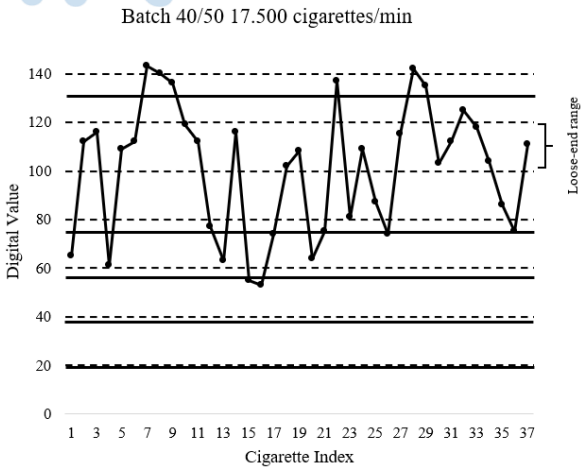

Figure 12. Example of Digital Value Obtained From Batch 40/50 17,500 cigarettes/min

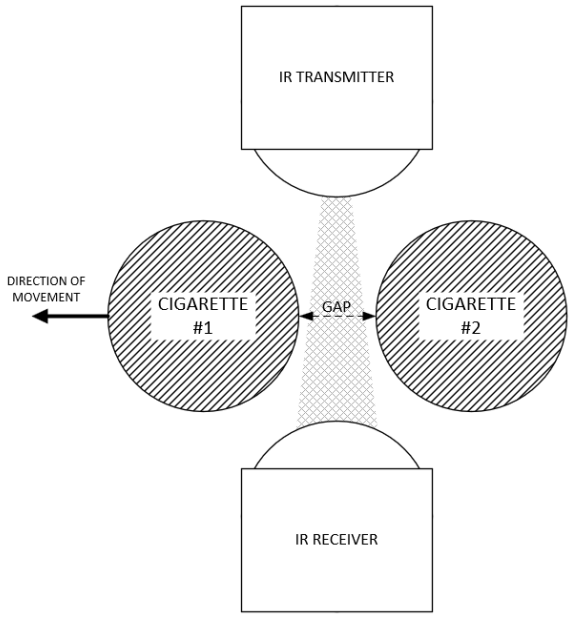

Figure 13. Illustration of Gap Between Cigarettes On Mechanical Rotator

Equation 2 is use to calculate the contrast properties of the measured signal.

$$CP = \frac{TP-P}{\bar{P}} \times 100\% \quad (2)$$

where,

CP = Contrast Properties Value (%)

$\overline{TP}$ = Average digital value of loose-end defective cigarette per batch

$\bar{P}$ = Average digital value of normal cigarette per batch

TABLE I. CONTRAST PROPERTIES AND ACCURACY VALUE OBTAINED FROM SEVERAL TEST BATCHES

No	Test Batches	Rotator Speed (cigarettes /min)	Contrast Properties (%)	Actual Loose-end Detected	Accuracy *(%)*
1.	49/50	10.000	76	1	100
2.	45/50	10.000	57	5	100
3.	40/50	10.000	55	14	71,4
4.	49/50	17.500	58	3	33,3
5.	45/50	17.500	48	5	100
6.	40/50	17.500	57	16	62,5

Table I shows the test results from several test batches. The average value of the contrast properties parameter is 58.5%, evenly distributed across test batches. The average value of the accuracy parameter is 90.5% at 10,000 cigarettes/min and 65.3% at 17,500 cigarettes/min, it has a tendency to decrease at faster speed and at larger amounts of loose-end defective cigarettes. Signal noise due to electromagnetic radiation generated by a motor controller seems to contribute to this.

IV. CONCLUSIONS

The proposed instrumentation system to detect loose-end defective cigarettes was successfully designed and tested using a specially built apparatus. Low-cost components and simple design were evidently effective and practical to obtain good performance parameters. This will give an opportunity to development of a complete fully automated detection and rejection of loose-end defective cigarettes machine at a much lower cost compared to existing expensive machines. This could be an alternative solution to help the small and home local industries in Indonesia to improve their cigarette product quality.

REFERENCES

[1] N. S. Fahira, A. Amira, and A. Firmansyah, "Profitability, liquidity, leverage, and firm risk: Evidence from Indonesian tobacco industry," *International Journal of Economics, Business and Accounting Research (IJEBAR)2*, vol. 4, no. 4, 2020.

[2] L. T. Tarmidi, "Changing Structure and Competition in THE Kretek Cigarette Industry," *Bull Indones Econ Stud*, vol. 32, no. 3, pp. 85–107, Dec. 1996, doi: 10.1080/00074919612331337038.

[3] T. Latinovic, C. Barz, A. P. Vadean, G. Sikanjic, and L. Sikman, "Adaptive intelligence system for a predictive process for the Industry 4.0 in Tobacco factory," in *Journal of Physics: Conference Series*, 2020. doi: 10.1088/1742-6596/1426/1/012019.

[4] Y. V. Hui and R. Wild, "Optimising production control of a maker-packer system in cigarette manufacture," *Journal of the Operational Research Society*, vol. 49, no. 8, 1998, doi: 10.1057/palgrave.jors.2600584.

[5] M. Husen, D. Gustopo, and D. I. Laksmana, "Product quality control using six sigma (DMAIC) methods to minimize wast in Bima Mandiri cigarette company Rembang, Pasuruan Regency," *Journal of Sustainable Technology and Applied Science (JSTAS)*, vol. 2, no. 2, 2021, doi: 10.36040/jstas.v2i2.3359.

[6] Buchegger J., Radzio, A., "Method and apparatus for testing the ends of cigarettes or the like," *US Patent US4486098A*,1984.

[7] Mitten, Robert T., Knight, Raymond J., Ripley, Robert L., "Cigarette detection and rejection device," *Patent CA1172932A*, 1984.

[8] Leslie, Elmer, and Payne, "Cigarette loose end detector-rejector mechanism," *US Patent US3485357A*, 1968.

[9] Merker, S, "System for detecting loose tobacco at cigarette ends," *US Patent US3729636A*, 1973.

[10] Lassiter, Wallace R., "Method and apparatus for detecting loose ends of cigarettes," *US Patent US5010904A*, 1989.

[11] Bolt, Reginald C., "Cigarette ends testing," *US Patent US4944314A*, 1987.

[12] E. Ni, S. Weizhong, W. Lisu, and Z. Desen, "Complete integrated single loose-end cigarette detection and rejection device," *Patent CN201494639U*, 2010.

[13] S. Feng, S. Siyang, and X. Shengping, "A real-time cigarettes counting and loose ends detection algorithm," *International Conference of Online Analysis and Computing Science (ICOACS)*, 2016.

[14] R. Ming *et al.*, "Cigarette loose-end detection method based on machine vision technology," *Patent CN102499471A*, 2012.

[15] R. Qu, G. Yuan, J. Liu, and H. Zhou, "Detection of cigarette appearance defects based on improved SSD model," in *ACM International Conference Proceeding Series*, 2021. doi: 10.1145/3501409.3501612.

AUTHOR GUIDELINES

1. Manuscript criteria

- The article has never been published or in the submission process on other publications.
- Submitted articles could be original research articles or technical notes.
- The similarity score from plagiarism checker software such as Turnitin is 20% maximum.
- For December 2021 publication onwards, Ultima Computing : Jurnal Sistem Komputer will be receiving and publishing manuscripts written in English only.

2. Manuscript format

- Article been type in Microsoft Word version 2007 or later.
- Article been typed with 1 line spacing on an A4 paper size (21 cm x 29,7 cm), top-left margin are 3 cm and bottom-right margin are 2 cm, and Times New Roman's font type.
- Article should be prepared according to the following author guidelines in this template. Article contain of minimum 3500 words.
- References contain of minimum 15 references (primary references) from reputable journals/conferences

3. Organization of submitted article

The organization of the submitted article consists of Title, Abstract, Index Terms, Introduction, Method, Result and Discussion, Conclusion, Appendix (if any), Acknowledgment (if any), and References.

- Title
  The maximum words count on the title is 12 words (including the subtitle if available)
- Abstract
  Abstract consists of 150-250 words. The abstract should contain logical argumentation of the research taken, problem-solving methodology, research results, and a brief conclusion.
- Index terms
  A list in alphabetical order in between 4 to 6 words or short phrases separated by a semicolon (;), excluding words used in the title and chosen carefully to reflect the precise content of the paper.
- Introduction
  Introduction commonly contains the background, purpose of the research, problem identification, research methodology, and state of the art conducted by the authors which describe implicitly.
- Method
  Include sufficient details for the work to be repeated. Where specific equipment and materials are named, the manufacturer's details (name, city and country) should be given so that readers can trace specifications by contacting the manufacturer. Where commercially available software has been used, details of the supplier should be given in brackets or the reference given in full in the reference list.
- Results and Discussion
  State the results of experimental or modeling work, drawing attention to important details in tables and figures, and discuss them intensively by comparing and/or citing other references.
- Conclusion
  Explicitly describes the research's results been taken. Future works or suggestion could be explained after it
- Appendix and acknowledgment, if available, could be placed after Conclusion.
- All citations in the article should be written on References consecutively based on its' appearance order in the article using Mendeley (recommendation). The typing format will be in the same format as the IEEE journals and transaction format.

4. Reviewing of Manuscripts

Every submitted paper is independently and blindly reviewed by at least two peer-reviewers. The decision for publication, amendment, or rejection is based upon their reports/recommendations. If two or more reviewers consider a manuscript unsuitable for publication in this journal, a statement explaining the basis for the decision will be sent to the authors within six months of the submission date.

5. Revision of Manuscripts

Manuscripts sent back to the authors for revision should be returned to the editor without delay (maximum of two weeks). Revised manuscripts can be sent to the editorial office through the same online system. Revised manuscripts returned later than one month will be considered as new submissions.

6. Editing References

- **Periodicals**
  J.K. Author, “Name of paper,” Abbrev. Title of Periodical, vol. x, no. x, pp. xxx-xxx, Sept. 2013.

- **Book**
  J.K. Author, “Title of chapter in the book,” in Title of His Published Book, xth ed. City of Publisher, Country or Nation: Abbrev. Of Publisher, year, ch. x, sec. x, pp xxx-xxx.

- **Report**
  J.K. Author, “Title of report,” Abbrev. Name of Co., City of Co., Abbrev. State, Rep. xxx, year.

- **Handbook**
  Name of Manual/ Handbook, x ed., Abbrev. Name of Co., City of Co., Abbrev. State, year, pp. xxx-xxx.

- **Published Conference Proceedings**
  J.K. Author, “Title of paper,” in Unabbreviated Name of Conf., City of Conf., Abbrev. State (if given), year, pp. xxx-xxx.

- **Papers Presented at Conferences**
  J.K. Author, “Title of paper,” presented at the Unabbrev. Name of Conf., City of Conf., Abbrev. State, year.

- **Patents**
  J.K. Author, “Title of patent,” US. Patent xxxxxxx, Abbrev. 01 January 2014.

- **Theses and Dissertations**
  J.K. Author, “Title of thesis,” M.Sc. thesis, Abbrev. Dept., Abbrev. Univ., City of Univ., Abbrev. State, year. J.K. Author, “Title of dissertation,” Ph.D. dissertation, Abbrev. Dept., Abbrev. Univ., City of Univ., Abbrev. State, year.

- **Unpublished**
  J.K. Author, “Title of paper,” unpublished. J.K. Author, “Title of paper,” Abbrev. Title of Journal, in press.

- **On-line Sources**
  J.K. Author. (year, month day). Title (edition) [Type of medium]. Available: http:// www.(URL) J.K. Author. (year, month). Title. Journal [Type of medium]. volume(issue), pp. if given. Available: http://www.(URL) Note: type of medium could be online media, CD-ROM, USB, etc.

7. Editorial Adress

Jl. Scientia Boulevard, Gading Serpong
Tangerang, Banten, 15811
Email: **ultimacomputing@umn.ac.id**

Paper Title

Subtitle (if needed)

Author 1 Name[1], Author 2 Name[2], Author 3 Name[2]
[1] Line 1 (of affiliation): dept. name of organization, organization name, City, Country
Line 2: e-mail address if desired
[2] Line 1 (of affiliation): dept. name of organization, organization name, City, Country
Line 2: e-mail address if desired

Accepted on mmmmm dd, yyyy
Approved on mmmmm dd, yyyy

***Abstract*—This electronic document is a "live" template which you can use on preparing your Ultima Computing paper. Use this document as a template if you are using Microsoft Word 2007 or later. Otherwise, use this document as an instruction set. Do not use symbol, special characters, or Math in Paper Title and Abstract. Do not cite references in the abstract.**

***Index Terms*—enter key words or phrases in alphabetical order, separated by semicolon (;)**

I. INTRODUCTION

This template, modified in MS Word 2007 and saved as a Word 97-2003 document, provides authors with most of the formatting specifications needed for preparing electronic versions of their papers. Margins, column widths, line spacing, and type styles are built-in here. The authors must make sure that their paper has fulfilled all the formatting stated here.

Introduction commonly contains the background, purpose of the research, problem identification, and research methodology conducted by the authors which been describe implicitly. Except for Introduction and Conclusion, other chapter's title must be explicitly represent the content of the chapter.

II. EASE OF USE

A. Selecting a Template

First, confirm that you have the correct template for your paper size. This template is for Ultima Computing. It has been tailored for output on the A4 paper size.

B. Maintaining the Integrity of the Specifications

The template is used to format your paper and style the text. All margins, column widths, line spaces, and text fonts are prescribed; please do not alter them.

III. PREPARE YOUR PAPER BEFORE STYLING

Before you begin to format your paper, first write and save the content as a separate text file. Keep your text and graphic files separate until after the text has been formatted and styled. Do not add any kind of pagination anywhere in the paper. Please take note of the following items when proofreading spelling and grammar.

A. Abbreviations and Acronyms

Define abbreviations and acronyms the first time they are used in the text, even after they have been defined in the abstract. Abbreviations such as IEEE, SI, MKS, CGS, sc, dc, and rms do not have to be defined. Abbreviations that incorporate periods should not have spaces: write "C.N.R.S.," not "C. N. R. S." Do not use abbreviations in the title or heads unless they are unavoidable.

B. Units

- Use either SI (MKS) or CGS as primary units (SI units are encouraged).
- Do not mix complete spellings and abbreviations of units: "Wb/m2" or "webers per square meter," not "webers/m2." Spell units when they appear in text: "...a few henries," not "...a few H."
- Use a zero before decimal points: "0.25," not ".25."

C. Equations

The equations are an exception to the prescribed specifications of this template. You will need to determine whether or not your equation should be typed using either the Times New Roman or the Symbol font (please no other font). To create multileveled equations, it may be necessary to treat the equation as a graphic and insert it into the text after your paper is styled.

Number the equations consecutively. Equation numbers, within parentheses, are to position flush right, as in (1), using a right tab stop.

$$\int_0^{r_2} F(r,\phi)\, dr\, d\phi = [\sigma r_2 / (2\mu_0)] \qquad (1)$$

Note that the equation is centered using a center tab stop. Be sure that the symbols in your equation have been defined before or immediately following the

equation. Use "(1)," not "Eq. (1)" or "equation (1)," except at the beginning of a sentence: "Equation (1) is ..."

D. Some Common Mistakes

- The word "data" is plural, not singular.
- The subscript for the permeability of vacuum μ_0, and other common scientific constants, is zero with subscript formatting, not a lowercase letter "o."
- In American English, commas, semi-/colons, periods, question and exclamation marks are located within quotation marks only when a complete thought or name is cited, such as a title or full quotation. When quotation marks are used, instead of a bold or italic typeface, to highlight a word or phrase, punctuation should appear outside of the quotation marks. A parenthetical phrase or statement at the end of a sentence is punctuated outside of the closing parenthesis (like this). (A parenthetical sentence is punctuated within the parentheses.)
- A graph within a graph is an "inset," not an "insert." The word alternatively is preferred to the word "alternately" (unless you really mean something that alternates).
- Do not use the word "essentially" to mean "approximately" or "effectively."
- In your paper title, if the words "that uses" can accurately replace the word using, capitalize the "u"; if not, keep using lower-cased.
- Be aware of the different meanings of the homophones "affect" and "effect," "complement" and "compliment," "discreet" and "discrete," "principal" and "principle."
- Do not confuse "imply" and "infer."
- The prefix "non" is not a word; it should be joined to the word it modifies, usually without a hyphen.
- There is no period after the "et" in the Latin abbreviation "et al."
- The abbreviation "i.e." means "that is," and the abbreviation "e.g." means "for example."

IV. Using the Template

After the text edit has been completed, the paper is ready for the template. Duplicate the template file by using the Save As command, and use the naming convention as below

ULTIMATICS_firstAuthorName_paperTitle.

In this newly created file, highlight all of the contents and import your prepared text file. You are now ready to style your paper. Please take note on the following items.

A. Authors and Affiliations

The template is designed so that author affiliations are not repeated each time for multiple authors of the same affiliation. Please keep your affiliations as succinct as possible (for example, do not differentiate among departments of the same organization).

B. Identify the Headings

Headings, or heads, are organizational devices that guide the reader through your paper. There are two types: component heads and text heads.

Component heads identify the different components of your paper and are not topically subordinate to each other. Examples include ACKNOWLEDGMENTS and REFERENCES, and for these, the correct style to use is "Heading 5."

Text heads organize the topics on a relational, hierarchical basis. For example, the paper title is the primary text head because all subsequent material relates and elaborates on this one topic. If there are two or more sub-topics, the next level head (uppercase Roman numerals) should be used and, conversely, if there are not at least two sub-topics, then no subheads should be introduced. Styles, named "Heading 1," "Heading 2," "Heading 3," and "Heading 4", are prescribed.

C. Figures and Tables

Place figures and tables at the top and bottom of columns. Avoid placing them in the middle of columns. Large figures and tables may span across both columns. Figure captions should be below the figures; table heads should appear above the tables. Insert figures and tables after they are cited in the text. Use the abbreviation "Fig. 1," even at the beginning of a sentence.

TABLE I. TABLE STYLES

Table Head	**Table Column Head**		
	Table column subhead	***Subhead***	***Subhead***
copy	More table copy		

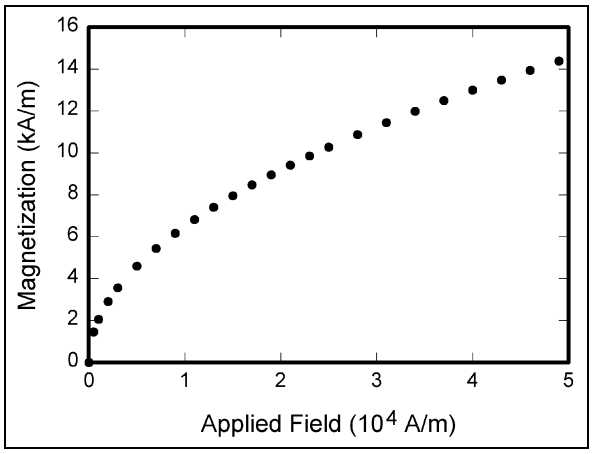

Fig. 1. Example of a figure caption

V. Conclusion

A conclusion section is not required. Although a conclusion may review the main points of the paper, do not replicate the abstract as the conclusion. A conclusion might elaborate on the importance of the work or suggest applications and extensions.

Appendix

Appendixes, if needed, appear before the acknowledgment.

ACKNOWLEDGMENT

The preferred spelling of the word "acknowledgment" in American English is without an "e" after the "g." Use the singular heading even if you have many acknowledgments. Avoid expressions such as "One of us (S.B.A.) would like to thank ... ." Instead, write "F. A. Author thanks ... ." You could also state the sponsor and financial support acknowledgments here.

References

The template will number citations consecutively within brackets [1]. The sentence punctuation follows the bracket [2]. Refer simply to the reference number, as in [3]—do not use "Ref. [3]" or "reference [3]" except at the beginning of a sentence: "Reference [3] was the first ..."

Number footnotes separately in superscripts. Place the actual footnote at the bottom of the column in which it was cited. Do not put footnotes in the reference list. Use letters for table footnotes.

Unless there are six authors or more give all authors' names; do not use "et al.". Papers that have not been published, even if they have been submitted for publication, should be cited as "unpublished" [4]. Papers that have been accepted for publication should be cited as "in press" [5]. Capitalize only the first word in a paper title, except for proper nouns and element symbols.

For papers published in translation journals, please give the English citation first, followed by the original foreign-language citation [6].

[1] G. Eason, B. Noble, and I.N. Sneddon, "On certain integrals of Lipschitz-Hankel type involving products of Bessel functions," Phil. Trans. Roy. Soc. London, vol. A247, pp. 529-551, April 1955. (*references*)

[2] J. Clerk Maxwell, A Treatise on Electricity and Magnetism, 3rd ed., vol. 2. Oxford: Clarendon, 1892, pp.68-73.

[3] I.S. Jacobs and C.P. Bean, "Fine particles, thin films and exchange anisotropy," in Magnetism, vol. III, G.T. Rado and H. Suhl, Eds. New York: Academic, 1963, pp. 271-350.

[4] K. Elissa, "Title of paper if known," unpublished.

[5] R. Nicole, "Title of paper with only first word capitalized," J. Name Stand. Abbrev., in press.

[6] Y. Yorozu, M. Hirano, K. Oka, and Y. Tagawa, "Electron spectroscopy studies on magneto-optical media and plastic substrate interface," IEEE Transl. J. Magn. Japan, vol. 2, pp. 740-741, August 1987 [Digests 9th Annual Conf. Magnetics Japan, p. 301, 1982].

[7] M. Young, The Technical Writer's Handbook. Mill Valley, CA: University Science, 1989.

UMN

UNIVERSITAS
MULTIMEDIA
NUSANTARA

ISSN 2355-3286

UMN
UNIVERSITAS
MULTIMEDIA
NUSANTARA

PRESS

Universitas Multimedia Nusantara
Scientia Garden Jl. Boulevard Gading Serpong, Tangerang
Telp. (021) 5422 0808 | Fax. (021) 5422 0800